BORON DETERMINATION IN BODY FLUIDS BY INDUCTIVELY COUPLED PLASMA OPTICAL EMISSION SPECTROMETRY AND INDUCTIVELY COUPLED PLASMA MASS SPECTROMETRY

A THESIS SUBMITTED TO
THE GRADUATE SCHOOL OF NATURAL AND APPLIED SCIENCES
OF
MIDDLE EAST TECHNICAL UNIVERSITY

BY

SELİN BORA

IN PARTIAL FULFILLMENT OF THE REQUIREMENTS
FOR
THE DEGREE OF MASTER OF SCIENCE
IN
CHEMISTRY

JANUARY 2010

Approval of the thesis;

BORON DETERMINATION IN BODY FLUIDS BY INDUCTIVELY COUPLED PLASMA OPTICAL EMISSION SPECTROMETRY AND INDUCTIVELY COUPLED PLASMA MASS SPECTROMETRY

submitted by **SELİN BORA** in a partial fulfillment of the requirements for the degree of **Master of Science in Chemistry Department, Middle East Technical University** by

Prof. Dr. Canan Özgen
Dean, Graduate School of **Natural and Applied Sciences** _____

Prof. Dr. Ahmet M. Önal
Head of Department, **Chemistry** _____

Prof Dr. O. Yavuz Ataman
Supervisor, **Chemistry Department, METU** _____

Examining Committee Members:

Prof. Dr. E. Hale Göktürk
Chemistry Department, METU _____

Prof. Dr. O. Yavuz Ataman
Chemistry Department, METU _____

Assoc. Prof. Dr. Nusret Ertaş
Faculty of Pharmacy, Gazi University _____

Prof. Dr. Mürvet Volkan
Chemistry Department, METU _____

Prof. Dr. G. İnci Gökmen
Chemistry Department, METU _____

Date: 19.01.2010

I hereby declare that all information in this document has been obtained and presented in accordance with academic rules and ethical conduct. I also declare that, as required by these rules and conduct, I have fully cited and referenced all material and results that are not original to this work.

Name, Last name: Selin Bora

Signature

ABSTRACT

BORON DETERMINATION IN BODY FLUIDS BY INDUCTIVELY COUPLED PLASMA OPTICAL EMISSION SPECTROMETRY AND INDUCTIVELY COUPLED PLASMA MASS SPECTROMETRY

Bora, Selin

M.S., Department of Chemistry

Supervisor: Prof. Dr. O. Yavuz Ataman

January 2010, 96 pages

Boron element plays an important role for our country since approximately 70% of the world's reserves are in Turkey. It is widely used in different areas of industry. Besides being vital for the plants, it is important also for human health. It has been shown that high boron exposure does not affect fertility negatively and also with an increasing boron exposure, risk of prostate and cervical cancers decreases. There are different opinions regarding health effects of boron. There are both positive and negative findings. Therefore, determination of boron in body fluids such as urine and blood is necessary to monitor exposed concentration level and its relation with diseases. Furthermore, these studies may contribute to define a reference value for safe maximum daily boron intake.

In this study, a method previously developed by our research group was applied for the determination of boron in urine samples. Urine and blood samples were collected from human subjects living or working in different regions of Balıkesir where boron reserves are located. While urine analysis was done by using Inductively Coupled Plasma Optical Emission Spectrometry (ICP-OES), due to lower concentrations of boron in blood, Inductively Coupled Plasma Mass

Spectrometry (ICP-MS) was used for blood analysis. A sensitive method was developed using ICP-MS.

Samples were digested in microwave oven by applying optimized digestion procedures. Indium (In) and Beryllium (Be) internal standards were spiked into the urine and blood samples, respectively. A sample introduction system containing no glass or silica surfaces was used in ICP-MS to eliminate boron memory effect. Two isotopes of the boron, ^{10}B and ^{11}B, were monitored during the study. Space charge effect due to Na^+ ion and carbon interference on B and Be signals was investigated in detail. Limit of Detection was 0.021 mg/L for ICP-OES and it was 2.2 µg/L for ICP-MS. The accuracies of the methods were checked by using NIST 1573a Tomato Leaves and BCR Human Hair certified reference materials for urine and blood, respectively.

Keywords: Boron determination, body fluids, ICP-OES, ICP-MS, memory effect, carbon interference.

ÖZ

VÜCUT SIVILARINDA ENDÜKTİF EŞLEŞMİŞ PLAZMA OPTİK EMİSYON SPEKTROMETRİ VE ENDÜKTİF EŞLEŞMİŞ PLAZMA KÜTLE SPEKTROMETRİ İLE BOR TAYİNİ

Bora, Selin

Yüksek Lisans, Kimya Bölümü

Tez Yöneticisi: Prof. Dr. O. Yavuz Ataman

Ocak 2009, 96 sayfa

Dünyadaki bor rezervlerinin yaklaşık %70'i Türkiye'de bulunduğundan, bor ülkemiz için önemli bir rol oynamaktadır. Bor, endüstrinin farklı alanlarında geniş bir kullanım alanına sahiptir. Bitkiler için hayati öneminin yanısıra, insanlar için de önemli bir elementtir. Yüksek bor maruziyetinin üretkenlik üzerinde olumsuz etkiler oluşturmadığı, ayrıca artan bor maruziyetiyle birlikte prostat ve rahim ağzı kanserine yakalanma riskinin azaldığı gösterilmiştir. Borun sağlık etkileriyle ilgili olarak farklı görüşler bulunmaktadır. Bu konuda olumlu ve olumsuz sonuçlar bulunmaktadır. Dolayısıyla, maruz kalınan düzeyi belirlemek ve bunu hastalıklarla ilişkilendirebilmek için idrar ve kan gibi vücut sıvılarında bor tayini yapmak gerekmektedir. Ayrıca bu araştırmalarda, güvenilir maksimum günlük bor alımı için referans değer belirlemek için katkı sağlanabilir.

Bu çalışmada, idrar örneklerinde bor tayini için grubumuz tarafından geliştirilen yöntem uygulanmıştır. İdrar ve kan örnekleri bor yataklarının bulunduğu Balıkesir'in farklı bölgelerinde yaşayan veya çalışan kişilerden toplanmıştır. İdrar örneklerinin analizi için Endüktif Eşleşmiş Plazma Optik Emisyon Spektrometri

(ICP-OES) kullanılırken, kandaki daha düşük derişimden dolayı kan örnekleri için Endüktif Eşleşmiş Plazma Kütle Spektrometri (ICP-MS) kullanılmıştır.

Örnekler, optimize edilen çözünürleştirme prosedürü uygulanarak mikrodalga etüvde çözünürleştirilmiştir. Indiyum (In) ve Berilyum (Be) iç standartları sırasıyla idrar ve kan örneklerine katılmıştır. ICP-MS cihazında hafıza etkisini ortadan kaldırmak için cam veya silika yüzey içermeyen bir örnek aktarma sistemi kullanılmıştır. Çalışma boyunca B elementinin iki izotopu da, ^{10}B ve ^{11}B, değerlendirilmiştir. Na^+ iyonunun yerel yük etkisi ile karbonun B ve Be sinyalleri üzerindeki girişim etkisi araştırılmıştır. Gözlenebilme sınırı ICP-OES için 0.021 mg/L iken, ICP-MS için 2.2 μg/L olarak hesaplanmıştır. Geliştirilen metotların doğruluğu idrar ve kan örnekleri için sırasıyla 1573a Tomato Leaves ve BCR Human Hair sertifikalı referans maddeleri kullanılarak irdelenmiştir.

Anahtar Kelimeler: Bor tayini, vücut sıvıları, ICP-OES, ICP-MS, hafıza etkisi, karbon girişim etkisi.

Dedicated to My Family...

ACKNOWLEDGEMENTS

I would like to express my deep appreciation and respect to my supervisor Prof. Dr. O. Yavuz Ataman for his endless guidance, support, encouragement, understanding, patience and suggestions throughout this study.

My special thanks to Dr. Sezgin Bakırdere not only for his guidance, patience and moral support during this study but also his sincere friendship.

I would like to thank to Yasin Arslan for his encouragement, guidance and friendship.

I want to thank to Assoc. Prof. Dr. Mehmet Korkmaz and Prof. Dr.Yalçın Duydu for providing the samples.

I am deeply grateful to Emrah Yıldırım, Pınar Akay, İlknur Demirtaş, Feriye Şenol, Üftade Muşkara, Şefika Eroğlu and Njaw Njie for their help and friendship. I also want to thank to Gamze Karaman, Seval Ataman, Erhan Özdemir and Mustafa Aydın for their help during sample preparation.

I would like to thank to Necati Koç for his help about technical issues.

Regarding TOC analysis, I should also thank to Saltuk Pirgalıoğlu for his help.

I would like to thank to TÜBİTAK for awarding scholarship during my second year of the master program.

Finally, my special thanks to my family for their trust, patience, support and love.

TABLE OF CONTENTS

ABSTRACT iv

ÖZ vi

TABLE OF CONTENTS x

LIST OF TABLES xiii

LIST OF FIGURES xv

LIST OF ABRREVIATIONS xvii

CHAPTERS

1. INTRODUCTION 1

1.1. Boron 1

1.1.1. Properties and Applications 1

1.1.2. Boron minerals and mining areas 3

1.1.3. Importance of Boron for Plants 5

1.1.4. Importance of Boron for Animals and Humans 6

1.2. Boron Determination Techniques 8

1.2.1. Molecular Spectrophotometry 8

1.2.2. Potentiometry 9

1.2.3. Neutron Activation Analysis (NAA) 9

1.2.4. Atomic Spectrometry 10

1.2.4.1. Inductively Coupled Plasma Optical Emission Spectrometry (ICP-OES) 12

1.2.4.2. Inductively Coupled Plasma Mass Spectrometry (ICP-MS) 15

1.3. Robustness Test for ICP-OES 17

1.4. Memory Effect in Plasma Techniques..... 18
1.5. Internal Standard Technique..... 20
1.6. Microwave Digestion..... 21
1.6.1. Working Principle of Microwave Oven..... 23
1.7. Aim of the Study..... 23
2. EXPERIMENTAL..... 24
2.1. Boron Determination in Urine Samples..... 24
2.1.1. Reagents and Samples..... 24
2.1.2. Apparatus and Materials..... 25
2.1.3. Microwave Digestion System..... 25
2.1.4. Inductively Coupled Plasma Optical Emission Spectrometer..... 26
2.2. Boron Determination in Blood Samples..... 27
2.2.1. Reagents and Samples..... 27
2.2.2. Apparatus and Materials..... 28
2.2.3. Microwave Digestion System..... 28
2.2.4. Inductively Coupled Plasma Mass Spectrometer..... 29
2.2.5. Total Organic Carbon Analyzer..... 31
3. RESULTS AND DISCUSSION..... 32
3.1. Determination of Boron in Urine Samples by ICP-OES..... 32
3.1.1. Optimization of ICP-OES Parameters..... 32
3.1.1.1. Optimization of Flow Rate of Coolant Argon..... 33
3.1.1.2. Optimization of Nebulizer Pressure..... 34
3.1.1.3. Optimization of Sample Solution Flow Rate..... 36
3.1.1.4. Optimization of the Flow Rate of Auxiliary Argon..... 37
3.1.2. Interference Effect of Fe on B Signals..... 39

3.1.3. Calibration Plot and Signals for Urine Analysis 40
3.1.4. Accuracy Check of the Method..... 44
3.2. Determination of Boron in Blood Samples by ICP-MS..... 45
3.2.1. Method Development with Borosilicate and Quartz Sample Introduction System 45
3.2.2. Method Development with PFA-Alumina Sample Introduction System 52
3.2.2.1. Effect of Be on Signal of ^{10}B..... 56
3.2.2.2. Solution Composition for Digestion of Blood Samples 57
3.2.2.3. Effect of Sodium on Signals of B and Be 58
3.2.2.4. Effect of Carbon on Signals of B and Be..... 61
3.2.2.5. Accuracy Check of the Method..... 69
3.2.2.6. Calculations for Boron Concentration in Blood..... 70
3.2.2.7. Boron Concentrations of the Urine and Blood Samples..... 72
4. CONCLUSIONS 87
REFERENCES..... 90

LIST OF TABLES

TABLES

Table 1. 1 Important boron minerals and their chemical formulas..... 3
Table 1. 2 Refined boron products and their B_2O_3 compositions. 4
Table 2. 1 Microwave Digestion Program for urine samples 26
Table 2. 2 Operating Parameters of ICP-OES..... 27
Table 2. 3 Microwave Digestion Program for blood samples..... 28
Table 2. 4 Operating Parameters of ICP-MS 30
Table 3. 1 Optimized parameters for Ar plasma 39
Table 3. 2 Analytical Figures of Merit for B with ICP-OES 43
Table 3. 3 Result of the Accuracy Check for ICP-OES..... 45
Table 3. 4 Analytical Figures of Merit for ^{11}B and ^{10}B with borosilicate and quartz sample introduction system. 51
Table 3. 5 Analytical Figures of Merit for ^{11}B with PFA-Alumina sample introduction system. 55
Table 3. 6 Analytical Figures of Merit of the sample for ^{11}B with PFA-Alumina sample introduction system. 56
Table 3. 7 % change of the ^{11}B, ^{10}B and ^{9}Be signals for different Na ion concentrations; N=2 59
Table 3. 8 Ratios of ^{11}B to ^{9}Be and ^{10}B to ^{9}Be and also their % changes for different Na ion concentrations; N=2 60
Table 3. 9 Concentrations of important ions in blood 61
Table 3. 10 First ionization potentials of some elements..... 62
Table 3. 11 ICPS of ^{11}B, ^{10}B and ^{9}Be with increasing sugar contents..... 62
Table 3. 12 % change of the ^{11}B, ^{10}B and ^{9}Be signals for different sugar contents. N=2 63

Table 3. 13 Ratios of ^{11}B to ^{9}Be and ^{10}B to ^{9}Be and also their % changes with increasing sugar contents. N=2 64
Table 3. 14 Result of the Accuracy Check for ICP-MS 69
Table 3. 15 Comparison of the corrected and uncorrected ICPS. 70
Table 3. 16 Boron concentrations of the urine samples from Bigadiç region 72
Table 3. 17 Boron concentrations of the urine samples from Bandırma region ... 73
Table 3. 18 Boron concentrations of the blood samples from Bandırma region ... 78
Table 3. 19 Group Statistics for urine samples from Bigadiç region 83
Table 3. 20 Independent-sample t-test results for two groups of urine samples from Bigadiç region 84
Table 3. 21 Group Statistics for urine samples from Bandırma region 84
Table 3. 22 Independent-sample t-test results for two groups of urine samples from Bandırma region 85
Table 3. 23 Group Statistics for blood samples from Bandırma region 85
Table 3. 24 Independent-sample t-test results for two groups of blood samples from Bandırma region 86

LIST OF FIGURES

FIGURES

Figure 1.1 Detailed view of plasma torch. 14
Figure 1. 2 The interface region of ICP-MS…..... 16
Figure 1. 3 Schematic of Quadrupole Mass Analyzer……. 17
Figure 3. 1 Optimization of the coolant flow rate using the power of 1.4 kW 33
Figure 3. 2 Optimization of the coolant flow rate using the power of 1.3 kW 34
Figure 3. 3 Optimization of the nebulizer pressure using the power of 1.4 kW ... 35
Figure 3. 4 Optimization of the nebulizer pressure using the power of 1.3 kW ... 35
Figure 3. 5 Optimization of sample solution flow rate 36
Figure 3. 6 Optimization of sample solution flow rate 37
Figure 3. 7 Optimization of the auxiliary gas flow rate using the power of 1.4 kW 38
Figure 3. 8 Optimization of the auxiliary flow rate using the power of 1.3 kW ... 38
Figure 3. 9 Calibration plot for B by ICP-OES, using conditions in Table 3.1 for urine analysis. 40
Figure 3. 10 Signals of B by ICP-OES. 41
Figure 3. 11 Signals of In by ICP-OES..... 41
Figure 3. 12 Signals of some standards and samples in duplicate..... 42
Figure 3. 13 Comparison of the standard addition and direct calibration techniques..... 43
Figure 3. 14 Plot of standard addition technique for B determination in NIST 1573a Tomato Leaves. 45
Figure 3. 15 Linear calibration plot for ^{11}B in deionized water. 46
Figure 3. 16 Signals of 10.0 ng/mL ^{11}B standard solution to show memory effect. 47

Figure 3. 17 Calibration plot for B prepared in 0.25% (w/v) mannitol and 0.10 M ammonia solution; ^{11}B was measured. 47
Figure 3. 18 Signal of 0.25% (w/v) mannitol and 0.10 M ammonia solution as a wash solution. 48
Figure 3. 19 Signal of 20 ng/mL ^{11}B in 0.25% (w/v) mannitol and 0.10 M ammonia solution. 48
Figure 3. 20 Calibration plot for ^{11}B using Indium as an internal standard in 1.0 M HNO_3. 49
Figure 3. 21 ^{11}B signals of the same 10.0 ng/mL boron standard solution; mannitol-ammonia mixture was used as a wash solution. 50
Figure 3. 22 Calibration plot for ^{11}B using ^{9}Be as an internal standard in 1.0 M HNO_3 51
Figure 3. 23 Calibration plot for ^{10}B using ^{9}Be as an internal standard in 1.0 M HNO_3. 52
Figure 3. 24 PFA spray chamber used in the study. 53
Figure 3. 25 Quartz torch with an alumina injector tube used in the study. 53
Figure 3. 26 Calibration plot for ^{11}B using ^{9}Be as an internal standard with PFA-Alumina sample introduction system. 54
Figure 3. 27 ^{11}B signals of calibration standards with PFA-Alumina sample introduction system. 55
Figure 3. 28 Signals at nominal mass 10, for various concentrations of Be. 57
Figure 3. 29 Calibration plot for C standards. 65
Figure 3. 30 Skimmer cones with (a) and without (b) C deposition. 67
Figure 3. 31 Sampler cones with (a) and without (b) C deposition 67

LIST OF ABRREVIATIONS

AAS	Atomic Absorption Spectrometry
AES	Atomic Emission Spectrometry
cps	count per second
CRM	Certified Reference Material
DIN	Direct Injection Nebulization
ET-AAS	Electrothermal Atomic Absorption Spectrometry
ICP-OES	Inductively Coupled Plasma Optical Emission Spectrometry
ICP-MS	Inductively Coupled Plasma Mass Spectrometry
ICPS	Integrated count per second
LOD	Limit of Detection
LOQ	Limit of Quantification
NAA	Neutron Activation Analysis
PE	Polyethylene

PFA	Perfluoroalkoxy
PP	Polypropylene
psi	pound per square inch
PTFE	Polytetrafluoroethylene
SRM	Standard Reference Material
RSD	Relative Standard Deviation
SIMS	Secondary Ion Mass Spectrometry
TIMS	Thermal Ionization Mass Spectrometry
TOC	Total Organic Carbon
UV	Ultra-violet

CHAPTER 1

INTRODUCTION

1.1. Boron

1.1.1. Properties and Applications

Boron is a metalloid with the atomic number 5; its symbol is B. It is located at 3A group of the second period on the periodic table. Atomic mass of B is 10.81 g/mol. ^{10}B and ^{11}B are the two stable isotopes of boron. Natural mixtures contain 19.9% ^{10}B and 80.1% ^{11}B by weight.

Boron is never found as a free element on earth and it occurs in nature in the form of borates due to its high affinity for oxygen [1].

Elemental boron exists in two forms: amorphous boron which is a brown powder and crystalline boron which is dark grey in color. Crystalline boron is a semiconductor at room temperature. Although elementary boron does not react with gaseous HCl, HBr or HI; it reacts with gaseous HF forming BF_3, which is quite volatile [2, 3].

Boron is an electron-deficient element, possessing a vacant p-orbital. It has only three valence electrons and forms three bond pairs leaving a p-orbital unfilled in the valence shell [4]. So, it is an electrophile and compounds of boron often behave as Lewis acids. Although boron forms three bonds in most cases; in compounds with hydrogen it may be pentavalent and also it can be divalent in some lower oxides such as BO [2].

^{10}B has a high thermal neutron capture cross section with a 3837 barns and this property has led its use in nuclear shielding and in neutron capture therapy for malignant tumors [4].

When chemical properties are considered, boron has some similar properties with aluminum in terms of valence. However, most of the boron's properties resemble those of silicon rather than aluminum [2].

Boric acid: Metaboric acid, HBO_2, and orthoboric acid or simply boric acid, H_3BO_3, are two known boric acids in the free state. H_3BO_3 is a very weak, monobasic acid that exists in the form of colorless crystals or a white powder and dissolves in water. Its dissociation constant is $K_a = 6.0x10^{-10}$. It acts as a Lewis acid by accepting a hydroxyl ion to form the borate anion.

$$B(OH)_3 + 2\ H_2O <—> B(OH)_4^- + H_3O^+$$

Boric acid reacts with polyhydric alcohols such as glycerol, mannitol or sorbitol and forms complexes which are stronger in the acidity than the boric acid itself [2, 4].

Boron compounds with different metals and ametals are widely used in the industry. The most important industries that use boron are detergent, glass, ceramic, agriculture and textile. These industries use approximately 80% of the total consumption by the year of 2001 [5]. In addition, boron compounds are used in medicine for the preparation of disinfectants and drugs, in the cosmetics, leather and paint industries, metallurgy, nuclear applications and as a fuel for rocket motors [2].

1.1.2. Boron minerals and mining areas

Geologic volcanic activity is the source of the boron. Important boron reserves of the world are in Turkey, USA and Russia. Approximately 70% of the boron reserves are found in Turkey. Therefore, boron has an important role in Turkey. Although tincal, colemanite and ulexite are found abundantly in the boron ores of Turkey; there are other boron minerals which are also very important for trade [6]. Names of the boron minerals and their compositions are listed in Table 1.1 below.

Table 1. 1 Important boron minerals and their chemical formulas

NAME	**FORMULA**
Kernite	$Na_2B_4O_7.4H_2O$
Tincalkonite	$Na_2B_4O_7.5H_2O$
Tincal	$Na_2B_4O_7.10H_2O$
Probertite	$NaCaB_5O_9.5H_2O$
Ulexite	$NaCaB_5O_9.8H_2O$
Colemanite	$Ca_2B_6O_{11}.5H_2O$
Meyerhofferite	$Ca_2B_6O_{11}.7H_2O$
Inyoite	$Ca_2B_6O_{11}.\ 13H_2O$
Pandermite	$Ca_4B_{10}O_{19}.7H_2O$
Inderite	$Mg_2B_6O_{11}.15H_2O$
Hydroboracite	$CaMgB_6O_{11}.6H_2O$
Boracite	$Mg_3B_7O_{13}Cl$
Ascharite	$Mg_2B_2O_5.H_2O$
Datolite	$Ca_2B_2Si_2O_9.H_2O$
Sassolite (natural boric acid)	$B(OH)_3$

In Turkey, whereas main tincal reserves are found in Eskişehir-Kırka, colemanite reserves are found in Kütahya-Emet (Espey & Hisarcık), Balıkesir - Bigadiç and

Bursa - Kemalpaşa (Kestelek). Reserves of the other important mineral ulexite place in Balıkesir- Bigadiç [5, 6].

Boron compounds are classified into 3 groups as untreated boron, refined boron and end products. Refined boron products compose the biggest part of the consumption. The refined boron products around the world and their B_2O_3 % are listed in Table 1.2.

Table 1. 2 Refined boron products and their B_2O_3 compositions

Product Name	**Formula**	**B_2O_3 (%)**
Borax pentahydrate	$Na_2B_4O_7.5H_2O$	47.8
Borax decahydrate	$Na_2B_4O_7.10H_2O$	36.5
Unhydrated borax	$Na_2B_4O_7$	69.3
Boric acid	H_3BO_3	56.5
Unhydrated boric acid	B_2O_3	100.0
Sodium perborate	$NaBO_3.4H_2O$	22.0
Sodium metaborate	$Na_2B_2O_4.4H_2O$	64.2
Sodium octaborate	$Na_2B_8O_{13}.4H_2O$	81.8

End products are produced from the untreated and refined boron. Their production requires high technologies. Essential end products include elemental boron, boron carbide (B_4C), boron nitride (BN) and alloys of boron with iron, nickel and cobalt.

Boron carbide is an extremely hard material and it has the ability to absorb neutrons. Boron nitride crystallizes both in hexagonal and cubic forms. The hexagonal form of boron nitride, BN, corresponds to graphite. Since it has a resistance to high temperatures, it is used as lubricant. Besides hexagonal form, the cubic variety (c-BN) is analogous to diamond. Its hardness is inferior only to diamond, but its thermal and chemical stability is superior [5].

1.1.3. Importance of Boron for Plants

Boron is an essential micronutrient for plants for the normal growth and development. It is absorbed as the undissociated boric acid from the soil [7] and accumulates in cell wall in this form [8]. It plays a key role in the cell wall, membrane effect, enzyme interactions and transportation of the important substances within the cells [4]. According to a study by *Çakmak and Romheld* roles of boron in the cell wall intactness and synthesis and also in plasma membrane integrity were well described [9]. For the proper cell wall function, continuous supplementation of B is required [8, 10].

Interaction of the boron compounds with different enzymes results in the inhibition, stabilization or stimulation. For example, boric acid inhibits the *urease* immobilized on a membrane. Inhibition of variety of enzyme systems by borate and boronic acid which is an alkyl or aryl substituted boric acid has been proposed [11].

Membrane uptake of a number of nutrients is inhibited by B deficiency. For example, in B-deficient plants, plasma membranes are highly leaky and lose their functional integrity [9]. As a result, deficiency of boron inhibits the growth of plant and reproductive plant parts [10], decreases the yield and further causes death, depending on the severity of deficiency [12]. Most rapid response to B depletion is the inhibition of root elongation.

For prevention of boron deficiency, boron containing fertilizers are manufactured. Many liquid formulations of borates are used as fertilizer. However, highly soluble boric acid in monoethanolamine is more economical.

Apart from boron deficiency, boron toxicity is an important problem that can limit the plant growth and crop yields [13]. High concentrations of boron in the soil are the reason for the toxicity. Among the potential sources of high soil B content, irrigation

water is the most important contributor. Symptoms of the excess boron may range from the necrosis of some plant organs to death of the whole plant depending on the extent of the toxicity [12].

1.1.4. Importance of Boron for Animals and Humans

Besides being an essential micronutrient for plants, boron is an important mineral in animal and human nutrition. Its essentiality for humans is still debated because of its undefined biochemical functions.

Humans may be exposed to boron through three primary sources:

- consumption of private, municipal, or commercial (bottled) drinking water,
- dietary consumption of crops and other foodstuffs,
- inhalation of boron compounds during mining, manufacturing, and other industrial processing.

Drinking water is the significant source of boron. Besides water, fruits, vegetables, legumes and nuts are rich in boron concentration. Boron functions in the metabolism of numerous other substances involved in life processes. By this way, it can positively affect the brain, skeleton and immune systems [14].

Boron enhances the maturation in the bones. According to the previous studies boron depletion causes abnormal calcium metabolism that affects the bone development [15, 16]. In addition, boron deprivation affects the frequency distribution of brain electrical activity in animals and reduces behavioral activation and mental alertness in humans [17]. Moreover, *Bai and Hunt* reported that antibody response of rats against bacterial agents decreases in boron deficiency [18].

Homeostatic mechanisms exist for B. In healthy individuals, boron is rapidly excreted in the urine, does not accumulate in tissues and is kept in trace amounts in blood. Ingested boron is converted into boric acid, H_3BO_3, abundantly and in lesser amount into $B(OH)_4^-$ anions. Then, after transportation throughout the body, most of them are excreted. *Sutherland et al.* reported that 85% of the daily boron exposure excreted via urine [19].

Although boron is found in the boric acid, H_3BO_3, and borate, $B(OH)_4^-$, forms in the body; exposed dose is calculated as elemental boron. The reason is boric acid and borate show similar dose effect with elemental boron [20].

According to a study by *Hunt* the signs of chronic B toxicity are poor appetite, nausea, weight loss, and decreased sexual activity, seminal volume and sperm count in humans [21].

Experiments on animals proposed that threshold toxicity effect of B, which is about 4500 mg boric acid per kg, cause testicular cell damage and atrophy in males [14]. Similar to *Nielsen*, *Ku et al. and Weir et al*. claimed that high doses of boron cause atrophy and finally degeneration of the organ in several animal species [22, 23]. However, *Şaylı et al.* conducted several field studies and observed no evidence that high boron exposure has negative effects on human fertility [24]. For the study, they compared the reproduction of the residents of the Turkish villages which are located in Bigadiç, Balıkesir. One village has high levels of boron in drinking water although the other has not. According to this study, evidence of fertility was birth of a living child. As a result, high boron exposure did not cause infertility problems [25, 26, 27].

Apart from the effect of boron on reproduction system, its effects on development were studied. Two studies reported that when exposed to higher doses of boron; skeletal malformations and cardiovascular defects were observed in mice, rats and rabbits [28, 29]. Conversely, according to a study by *Nielsen* high doses of boron did not affect the development negatively [14].

On the other hand, *Cui et al.* proposed that boron and borates may show anticarcinogenic properties [30]. According to the results of the studies by *Cui et al.* and *Zhang et al.* as dietary intake of boron increases, the risk of prostate cancer decreases [30, 31]. Recent studies, in which our research group has made contributions, have proposed that high levels of boron exposure decrease the risk of cervical cancer-related pathological findings [32]. In this study, effect of adverse cytological findings in cervical smears of the women living in boron rich and boron poor regions were investigated. Regions are located in Bigadiç town of Balıkesir. In boron-rich region, women are exposed to boron through drinking water, foods which are grown in these areas and also during bathing. Cervical smears of the women from both regions were examined and results showed that women live in boron rich region were free of cervical malignancy although others had cytopathological interpretations. Moreover, according to a new study (*Korkmaz et al*., not published), as boron exposure increases, tendency of prostate enlargement decreases.

WHO suggested the acceptable safe range of B intake for adults between 1 to 13 mg/day considering both human and animal research data [33].

1.2. Boron Determination Techniques

1.2.1. Molecular Spectrophotometry

Molecular spectrophotometry techniques include colorimetry and fluorimetry for boron determination. Colorimetry based on the reaction of B with color forming reagents. Azomethine-H [34], curcumin and carmine [35] are the commonly used organic dyes which produce colored complexes with B. Among them, azomethine-H method is the most commonly used one. This method is based on the formation of a colored complex with boric acid at pH 5.1 and this complex has a 420 nm absorption maximum. It is a more reliable, fast, simple and sensitive method that suffers less

interference than other colorimetric methods [36]. In addition, hazardous chemicals are required for curcumin and carmine methods.

Fluorimetry uses the approach of formation of fluorescent complexes of B and the measurement of fluorescence induction at a specific wavelength. Alizarin Red S [37], chromotropic acid and dibenzoylmethane-isobutyl methyl ketone are the chemicals that form fluorescent compounds with B. Although this method is more sensitive than colorimetric methods, it suffers interferences from a number of chemical species. In addition, it is sensitive to pH and temperature.

Therefore, interference problems, sensitivity to pH and rather low sensitivity limit the application of molecular spectrophotometric techniques for boron determination.

1.2.2. Potentiometry

Boron determination by this technique requires the separation of B from the sample matrix, treatment with HF and then formed tetrafluoroborate ion (BF_4^-) is measured potentiometrically with a suitable BF_4^- selective electrode [38]. Since sample matrix is a big problem for this technique, it has not been widely used.

1.2.3. Neutron Activation Analysis (NAA)

In this technique, the sample is bombarded with a beam of thermal neutrons and neutron-capture reaction occurs. This reaction which involves only the ^{10}B isotope is as follows:

$$^{10}B + \text{neutron} \rightarrow {}^{7}Li + \alpha \text{ particles (2.31 MeV)} + \text{gamma ray (478 KeV)}$$

NAA requires a nuclear reactor to produce thermal neutrons for converting isotope(s) of interest in a sample to radioisotopes. B determination by NAA is based on the

measurement of one of the products of this reaction. The technique which uses α particles is called neutron capture radiography while that uses gamma ray is called prompt-γ neutron activation analysis [39].

The advantages of NAA are being a non-destructive method and having low detection limits. However, it needs a nuclear reactor that is not always easy to access.

1.2.4. Atomic Spectrometry

For boron determination many atomic spectrometry techniques such as Atomic Absorption Spectrometry (AAS), Atomic Emission Spectrometry (AES), Electrothermal Atomic Absorption Spectrometry (ET-AAS), Inductively Coupled Plasma Optical Emission Spectrometry (ICP-OES), Inductively Coupled Plasma Mass Spectrometry (ICP-MS), Thermal Ionization Mass Spectrometry (TIMS) and Secondary Ion Mass Spectrometry (SIMS) are employed.

AAS and AES techniques for B determination have relatively poor sensitivity [40] and also separation and preconcentration of B from sample matrix is often needed [41]. Furthermore, memory effects and interference problems are serious in these techniques.

ET-AAS has poor detection limits without the use of chemical modifiers. According to a study by *Luguera et al*. the reason is the inefficient thermal dissociation of B-containing species and memory effect problems due to interaction of analyte with carbon surface [42].

Due to lack of adequate sensitivity, memory effect problem and time-consuming sample preparation procedures; the techniques mentioned above have not been used widely for boron determination.

Besides the flame atomic spectrometry, plasma source techniques are also used for B determination. With the development of ICP-OES, problematic elements that include B can be detected. ICP-OES has low detection limits, large linear range and multi-element detection capability. The detection limit and precision of ICP-OES for B are better than all previous techniques mentioned above. One disadvantage is the iron interference for B determination. Iron interferes with the two most sensitive B lines at 249.773 nm and 249.678 nm in this technique if the sample has high iron concentrations. Fe at 249.782 nm interferes with B signal at 249.773 nm while Fe at 249.653 nm affects B signal at 249.678 nm. Moreover, for low trace amount of boron memory effect problem can be encountered [43].

Other plasma technique for boron determination is ICP-MS. It is preferred to ICP-OES [44] due to its higher sensitivity, lower detection limits, multi-element capability with a high speed scanning and simultaneous measurements of total B concentrations and B isotope ratios (^{11}B to ^{10}B). In addition, its capability to carry out B determination by isotope dilution method which is considered the most precise technique for quantitative analysis make this method unique. Drawbacks of ICP-MS are the spectral interference and memory effect problems. Spectral interference of ^{12}C peak on the ^{11}B signal can be a problem for the samples that contains high levels of organic carbon. According to the result of the study by *Evans and Krahenbuhl* signal of ^{11}B was affected significantly from ^{12}C in microwave digests of biological materials when analysis was performed in the low resolution mode that is usual for quadrupole MS instruments [45].

TIMS is the another plasma technique for the determination of B. This method has been used for isotopic determination of BO_2^+ or BO_2^- salts of Na, Cs or Rb [46]. It has high accuracy and precision. However, laborious sample preparation steps and long analysis times are the disadvantages of TIMS. So, it is less desirable for routine B determination.

The last plasma technique for boron determination is the SIMS. In contrast to other plasma techniques using SIMS B and its isotopic ratio in solid samples can be determined [47]. In this technique, energetic primary ion beam causes sputtering of the surface atoms from the small area of the sample. Then, secondary ions generated from the sample at mass 10 or 11 are detected by mass analyzer. Drawbacks of this method are high cost, difficulty in determining absolute B concentration due to different matrices that may provide different ion yield, poorer resolution than TIMS and difficulty in the analysis of volatile phases of B [48].

Evans et al. compared the photometry - azomethine-H, fluorimetry - carminic acid, ICP-OES and ICP-MS techniques for boron determination in terms of recovery and precision [44]. Biological samples were analyzed after microwave digestion. Good recoveries were obtained with all techniques except fluorimetry. Azomethine-H method was reliable only for the determination of high boron content. Finally, both ICP-OES and ICP-MS techniques gave the best precision.

1.2.4.1. Inductively Coupled Plasma Optical Emission Spectrometry (ICP-OES)

ICP-OES is composed of two main parts. ICP is the source of ionization while OES is for detection and quantification. The heart of an ICP-OES is the plasma which is an ionized gas at a temperature of several thousands Kelvin. Sample is destroyed completely by this very high temperature in the plasma. Formed atoms and ions are then excited to emit electromagnetic radiation. This radiation appears in the ultraviolet and visible range of the spectra. Finally, electromagnetic radiation is separated according to wavelengths by diffractive optics and intensities are measured with a detector [49].

Liquid sample is introduced to the system by a nebulizer, its function is to convert an aqueous sample into an aerosol by means of argon gas. Before reaching to the

plasma, coarse aerosols from nebulizer pass to the spray chamber for production of fine aerosols with the ideal particle size.

Plasma is composed of positive ions, electrons and neutral species of an inert gas, generally argon. Radio frequency (RF) power is supplied through the load coil which is made of copper. Power is in the range of 0.5 – 1.5 kW at a frequency of 27 or 40.68 MHz. Applied power causes an oscillating magnetic field inside the torch and outside the load coil. Then, with the help of the spark added from a Tesla coil free electrons are produced. Tesla coil is attached to the outside of the torch with a piece of copper wire. Accelerated free electrons cause collisions with atoms and molecules in order to ionize the argon gas.

$$Ar + e^- \rightarrow Ar^+ + 2e^-$$

The homogeneous magnetic field is important for the optimal coupling efficiency to the plasma [49, 50].

Plasma is not in thermodynamic equilibrium. The temperature of the plasma is approximately between 6000 and 10 000 K. It is about 10 000 K in the ring-shaped zone inside the load coil to which the energy of the coil is coupled.

Torch on which plasma is formed consists of three concentric tubes. These are outer, middle and injector tubes and generally are made from quartz. The argon gas for cooling the outer tube from melting is called *coolant*. This gas is also used to form the plasma for most designs so it is frequently referred to as *plasma gas*. It flows between the outer and the middle tubes at a flow rate of 12-20 L/min. The task of the *auxiliary gas* which flows between the middle tube and injector tube is to change the position of the base of the plasma relative to the injector tip if necessary. The range of the auxiliary flow rate is between 0.1 and 2.0 L/min. Lastly, argon gas that carries the aerosol is called *carrier gas* or *nebulizer gas*. The speed of the carrier gas flow has an influence on the residence time of the aerosol in the plasma. Low carrier gas flow is preferred for the aerosol to penetrate into the plasma. Typical carrier gas

flows are from 0.3 to 2.0 L/min [49, 51]. The schematic of an ICP torch is shown in Figure 1.1.

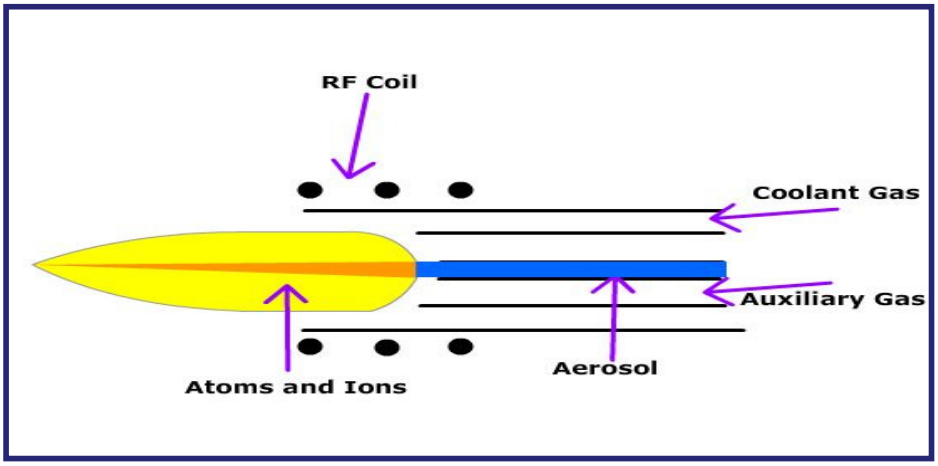

Figure 1. 1 Detailed view of plasma torch

ICP-OES has several advantages over other spectrometric techniques such as AAS, AES and ET-AAS. These advantages are as follows:

- Low detection limits (ng/mL range)
- Multi-element analysis
- Wide linear dynamic range
- Limited chemical interferences
- High sensitivity

Plasma Viewing

Spectrometer can view the plasma from two geometric directions: from the side (*radially*) or lengthways (*axially*).

Axial viewing: Instruments with a horizontal torch design have an axial viewing. Axial viewing improves the sensitivity and limit of detection. The limit of detection is lowered due to a greater number of excited atoms and ions are viewed. On the other hand, disadvantage of axial viewing is the increase in both spectral and non-spectral interferences [49].

1.2.4.2 Inductively Coupled Plasma Mass Spectrometry (ICP-MS)

ICP-MS is the most commonly used trace element technique for multi-element determinations today. As compared with ICP-OES, besides its fast multi-element characteristics, wider linear dynamic range, minimum chemical interferences, lower detection limits and ability to determine isotopic ratios are additional advantages of ICP-MS.

ICP part is the same with ICP-OES. However, MS part separates the ions according to mass-to-charge ratio while OES uses emitted photons to analyze the sample. After formation of the ions in the plasma, ions are directed into the mass spectrometer through the interface region. This region includes two metallic cones, sampler and skimmer cone. They are generally made from nickel due to its high thermal conductivity, resistance to corrosion and robust nature. Cones have small orifices (0.6-1.2 mm) to allow the ions to pass through to the ion optics. Due to these small orifices, no more than 0.2% (w/v) total dissolved solids are recommended for best performance and sensitivity. Otherwise, blockage in the orifices occurs and this causes lower sensitivity. The region between the sampler and skimmer cone is maintained at a moderate pressure of 1-2 Torr while pressure behind the skimmer

cone is at approximately 10^{-6} Torr. Vacuum is maintained by means of a turbomolecular pump. The role of the interface region is important since the ions must be transported efficiently to the mass analyzer. The interface region of ICP-MS is shown in Figure 1.2.

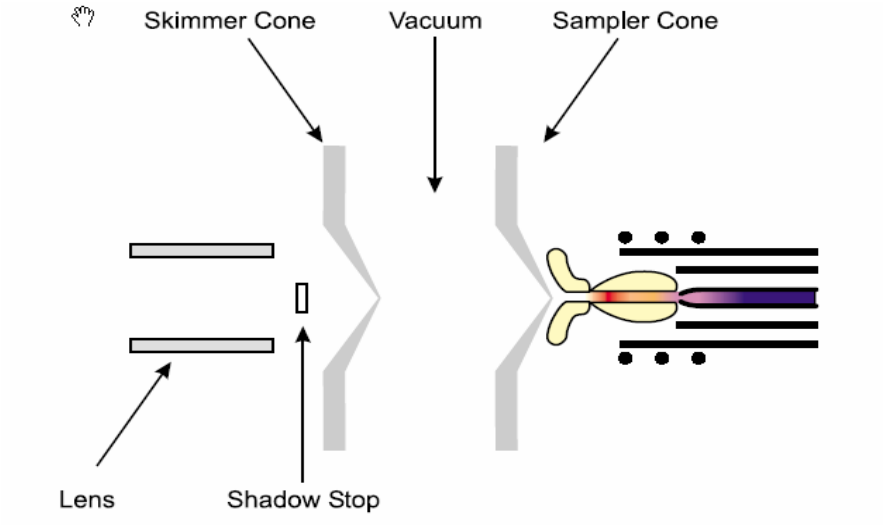

Figure 1. 2 The interface region of ICP-MS [52]

Ions extracted from the interface region are then focused into the mass analyzer by a series of electrostatic lenses. These lenses also prevent reaching of photons, particulates and neutral species to detector. Ion beam passes through the mass spectrometer after exiting ion optics. Quadrupole type mass analyzer separates analyte ions with a particular mass-to-charge ratio. In multi-element determination, ions are processed either simultaneously or sequentially depending on the design of the mass spectrometer. Then, ions reach the detector which is an electron-multiplier. Analyte ions are converted to electrical signal at detector.

Quadrupole mass analyzer consists of four cylindrical stainless steel rods of the same length and diameter. It operates by both direct current (DC) field and a time-dependent alternating current (AC) of radio frequency applied on opposite pairs of these four rods. In order to allow the selected mass to pass through detector, for each

pair of rods optimum AC/DC ratio is adjusted [51, 53]. The schematic of quadrupole mass analyzer is given in Figure 1.3.

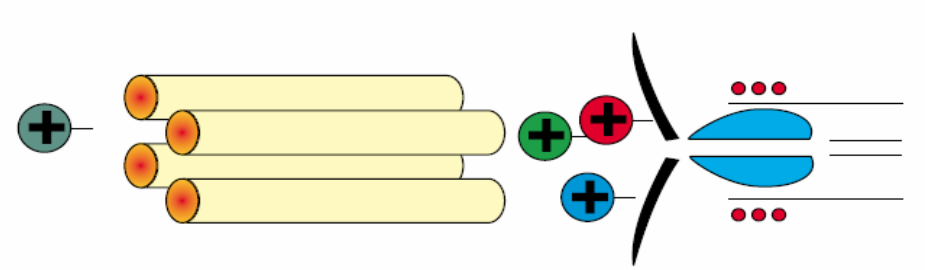

Figure 1. 3 Schematic of Quadrupole Mass Analyzer [52]

1.3. Robustness Test for ICP-OES

A robust system can tolerate small changes without affecting the line intensity of the analyte. More reproducible results are obtained when robust conditions are used.

In ICP, analyte species are transformed into atoms or ions. After atomization step, species are excited and then ionized. Neutral atoms give atomic lines whereas singly ionized atoms give the ionic lines. The ratio of the ionic to atomic line intensities of the same element allows an evaluation of the departure from local thermodynamic equilibrium (LTE) of the plasma. The Saha equation determines the ratio of ion to atom population for a species as a function of ionization temperature. Closeness to this equilibrium increases the atomization, excitation and ionization efficiency indicating the robust plasma conditions [54, 55].

To obtain a robust system, atomization and ionization processes are optimized by using Mg II 280.270 nm / Mg I 285.213 nm line intensity ratio. In this notation, Mg II refers to ionic line while Mg I refers to atomic line. According to a study by *Mermet* intensity ratio above 10 indicates the optimized conditions of ICP [56].

However, for axial viewing of ICP, this ratio will be lower than the radial viewing because in axial viewing both atomic and ionic line emission zones are probed by the collimating system. Therefore, intensity ratio can shift to 4 for axial viewing [54].

Selection criteria of the Mg as a test element are as follows;

- Closeness of the excitation energies of the atomic and ionic lines.
- Ionic line of Mg is very sensitive to parameter changes (little effect on this line changes the ratio).

Ionic to atomic line ratio can be increased by changing the values of operating parameters of ICP-OES to obtain robust system. Power, carrier gas flow rate and internal diameter of the injector are the important parameters [56]. High power (>1.4 kW), low carrier gas flow rate (<0.6 L/min) and large internal diameter of the injector provide bigger ratio to obtain more robust system. So, apart from power, residence time is also important. As the residence time increases, system will be more robust.

1.4. Memory Effect in Plasma Techniques

In boron determination studies, base line is elevated due to retainment of boron on glass surfaces. This situation affects further readings and causes errors. It is called memory effect [12]. This problem is more important for ICP-MS due to its more sensitive property.

Sun et al. explained the reason of memory effect as the reaction of B with the walls of the sample introduction system, especially the spray chamber, which is usually made of borosilicate glass or quartz [57].

In addition, *Al-Ammar et al.* theoretically characterized the mechanism of the problem [58]. According to them, volatilization of boron as boric acid from the solution layer and adhesion inside surface of the spray chamber is the reason of the memory effect. They proposed that boron should exist as boric acid in the solution since solution is prepared in a strong oxidizing nitric acid which decomposes the sample that will be analyzed. Also, boric acid is 99.93% undissociated even at pH 6 with its low dissociation constant, pKa=9.14. So, boric acid can volatilize from the aqueous layer and causes memory effect.

For the elimination of memory effect, many different techniques were proposed and tested. Some researchers reduce memory effect by long wash-out times [59]. Dilute nitric acid was one of the rinse solutions. *Evans and Krahenbuhl* suggested the using of sodium fluoride (NaF) as a wash solution [45]. They assume that excess fluoride forms complex with borate which is adsorbed onto the introduction system parts. After its formation, stable boron trifluoride is washed out. After introducing 100 ng/mL boron solution for 2 min, memory effect is eliminated by rinsing with slightly acidified 2 mg/mL NaF solution for 60 s. But for higher concentration of boron solution, rinse time increases. *Al-Ammar et al.* used ammonia gas to form non-volatile ammonium-borate [58]. Ammonia solution is introduced simultaneously with the sample solution into the spray chamber and this completely eliminates the boron memory effect.

Sun et al. minimized the memory effect by adding mannitol to the sample and flush solutions in a system that uses ultrasonic nebulizer [57]. The reason of the usage of mannitol is it can form very stable boron – mannitol complexes.

Direct Injection Nebulization (DIN) system was used by *Bellato et al.* to reduce memory effect and to improve the efficiency of the system [60]. The DIN system they use involves a computer controlled valve to transfer the sample into a capillary located inside the torch. Aerosol forms with the help of argon at the top of the torch.

Since this system does not include spray chamber as others, memory effect problem is minimized. Other advantage of this system is that aerosol transport efficiency is near 100%.

In literature, another solution to eliminate the memory effect is to use mannitol-ammonia mixture as both diluent and wash solution. All of the standards and samples included 0.25% (w/v) mannitol and 0.1 M ammonia. Also, 0.25% (w/v) mannitol and 0.1 M ammonia solution was prepared separately as wash solution. It was introduced for 1 min after each standard and sample. This wash solution helps to decrease the signal to the original blank signal. Furthermore, addition of 0.25% (w/v) mannitol and 0.1 M ammonia into the samples enhance the signals with respect to the solution prepared only in water, only in nitric acid and only in ammonia [61].

1.5. Internal Standard Technique

The aim of using the internal standard is to control the non-spectroscopic matrix effect and correct signal instability results from the instrumental shifts. Since plasma is not in a thermodynamic equilibrium, signals fluctuate with varying temperatures. When internal standard is used; ratio of analyte signal and the internal standard signal gives the correct value even the temperature of the plasma varies momentarily.

For boron determinations by ICP-OES, Indium (In) is suitable as an internal standard. Closeness of the wavelength of the internal standard to that of analyte is important. While B is viewed at 249.773 nm, In is monitored at 230.606 nm.

In ICP-MS, the main point for choosing an internal standard is the closeness of the mass number and similarity in ionization potential between the internal standard and the analyte [62]. So, Beryllium (Be) is a suitable internal standard for boron determination in ICP-MS since its mass is very close to boron (^{9}Be, $^{10\text{-}11}$B).

Moreover, ionization potential of Be is 9.3 eV while that of B is 8.3 eV. Most of the researchers use Be as an internal standard for their boron determination studies for different samples [45, 61, 63].

Apart from Be, Rhodium (^{103}Rh) is also used as an internal standard in ICP-MS studies for boron determination [64]. Ionization potential of Rh is 7.5 eV. However, Be is preferred to Rh in general.

Although the fact that most of the researchers use Be for boron determination studies, *Al-Ammar et al.* proposed that Be is not a suitable internal standard if the sample contains high amount of carbon [65]. They studied the non-spectral interference effects of carbon by charge transfer reaction and found that carbon enhances the signals of ^{11}B and ^{9}Be differently. According to the study, increase for the Be signals was less than that for B signals with varying carbon concentrations. This difference in the magnitude of the signal enhancement is the reason for the suggested failure of using Be. Moreover, they indicated the effectiveness of Rh, which has an ionization potential of 7.5 eV, as an internal standard for boron determination.

In addition, *Evans and Krahenbuhl* mentioned that usage of Be as an internal standard for ICP-MS may cause errors in the observed B/Be ratios when the acidities of the samples are different from each other [44].

1.6. Microwave Digestion

Today, complete sample dissolution is required by many instrumental techniques before analysis. Different decomposition techniques are used for sample preparation. These techniques include dry ashing, fusion and wet digestion with different acid mixtures in an open vessel on hot plate at atmospheric pressure or in closed vessels

by using microwave heating and high pressure (microwave digestion). Among them dry ashing and wet digestion techniques are generally slow and time-consuming. Furthermore, these techniques are open to sample loss by volatilization and contamination during the process [66]. However, microwave digestion prevents sample loss and contamination since it is a closed vessel system. In addition, increased temperature above the boiling points of the mineral acids enhances the oxidizing power of the acids that allow for the complete decomposition of matrix components. Apart from them, acid consumption is reduced in microwave-digestion [67].

At the end of the microwave digestion, sample matrix is completely destructed. Organic parts are converted to inorganic materials [68]. If biological samples such as blood are analyzed by ICP-MS, microwave digestion is necessary because undigested blood has a high content of organic compounds which cause problems with nebulizer and carbon deposition on the cones of the ICP-MS [69].

Nitric acid is commonly used mineral acid in microwave digestion. However, according to a study by *Wurfels et al.* some species such as aromatic proteins show resistance to complete oxidation by nitric acid and result in the formation of several resistant organic decomposition products which are identified as nitrobenzoic acids (NBA) [70]. These products can increase the residual carbon content (RCC) for digested samples. To deal with this problem, additional oxidants such as perchloric acid, sulfuric acid, hydrogen peroxide and hydrochloric acid are used in the literature. Hydrogen peroxide (H_2O_2) is used to destroy residual NBA compounds [66].

1.6.1. Working Principle of Microwave Oven

Microwave radiation results in the molecular motion by migration of ions and rotation of dipoles. However, it does not cause any molecular structure changes. Microwave energy is absorbed by the sample by two mechanisms; *ionic conduction* and *dipole rotation*. Ionic conduction is defined as the conductive migration of dissolved ions in the applied electromagnetic field. Ionic migration is the flow of current which results in heat production because of resistance to ion flow. Ion concentration, ion mobility and solution temperature are the parameters that affect ionic conduction. Molecules of sample with permanent or induced dipole moments align due to electric field. This is called as dipole rotation. When the field is removed, thermal energy is released and molecules return to disorder. Efficiency of the heating by dipole rotation mechanisms depend on the temperature and viscosity of the sample [71].

For the effectiveness of microwave system, reflective metals as construction materials, transparent vessels for the low-loss of energy and absorptive samples should be used [71].

1.7. Aim of the Study

The purpose of this study was to apply the developed method for analyzing urine samples by using ICP-OES and develop a sensitive analytical method for determination of boron in blood by ICP-MS. For this study, blood and urine samples were collected from the human subjects exposed to high boron. Reasonably high number of samples was analyzed by using developed methods to deduce reliable conclusions. Since there is no safe upper boron intake value; results can be helpful to determine a reference value. Results can also be used to refute the European Unions thesis which claims “boron is a toxic element.”

CHAPTER 2

EXPERIMENTAL

2.1. Boron Determination in Urine Samples

2.1.1. Reagents and Samples

1000 mg/L boron solution which was prepared from boric acid (Merck) in 1.0% (v/v) HNO_3 was used as the stock solution. Standard solutions were prepared in 1.0 M distilled HNO_3 by diluting the stock solution with 18 M Ω.cm deionized water from Millipore Milli-Q Water Purification System. For distillation of the analytical grade 65% (w/w) HNO_3 (Merck), the Berghof Acid Distillation System was used. Boron concentrations of the calibration standards were 0.10, 0.25, 0.50, 1.0, 2.0 and 5.0 mg/L.

Urine samples were collected from two different regions of Balıkesir, Bigadiç and Bandırma. Samples were divided into two groups which were Control and Study Group for both regions. For the samples from the Bigadiç region while Study Group involved the urine samples of subjects residing in the boron mining area, Control Group included urine samples from subjects living far from this area. On the other hand, Study Group of the Bandırma region consisted of the urine samples of donors working in boric acid factory whereas Control Group consisted of the urine samples of subjects living in the area where the factory is located but not working in factory.

Collected urine samples were stored in deep-freeze before analysis.
Stock solution of 1000 mg/L Indium (In) (High Purity) in 2.0% HNO_3 was used as the internal standard. Concentration of indium in all standard solutions and samples

was adjusted to 10.0 mg/L. 1.0 M HNO_3 solution was used as wash solution between each standard and sample during the analysis.

Accuracy of the method was controlled by using NIST 1573a Tomato Leaves as a standard reference material.

2.1.2. Apparatus and Materials

All of the solutions were prepared by using 100-1000 µL and 500-5000 µL range Eppendorf micropipettes. To prevent the possible boron contamination from the glass surface, Polypropylene (PP) volumetric flasks were used for the preparation of solutions. Then, solutions were stored in the polyethylene containers which were kept in refrigerator. For digestion of the sample, Polytetrafluoroethylene (PTFE) digestion bombs were used.

Before usage, all the labware were immersed in 10.0% (v/v) HNO_3 cleaning solution for at least overnight. The labware was then rinsed with deionized water and left to dry in a clean environment.

2.1.3. Microwave Digestion System

Milestone Ethos PLUS microwave dissolution system with a 10 digestion bombs set was used for digestion of the urine samples. 5.0 mL of sample were transferred into PTFE digestion bomb and 5.0 mL of distilled concentrated HNO_3 were added. Sample was digested in microwave oven. The applied program is given below.

Table 2. 1 Microwave Digestion Program for urine samples

Time	Temperature
3 min	20 ^{o}C → 100 ^{o}C
5 min	100 ^{o}C
3 min	100 ^{o}C → 150 ^{o}C
5 min	150 ^{o}C
3 min	150 ^{o}C → 180 ^{o}C
5 min	180 ^{o}C

Duplicate sample aliquots were digested separately. After digestion step, Indium (In) standard solution was spiked as an internal standard and sample was brought to a 25.0 mL final volume with de-ionized water in a polypropylene volumetric flask.

2.1.4. Inductively Coupled Plasma Optical Emission Spectrometer

For this study, Leeman Labs Inc. DRE (Direct Reading Echelle) with an axial view configuration Inductively Coupled Plasma Optical Emission Spectrometer was used. Determination of the elements was done sequentially with this instrument.

Best signal was obtained with 249.773 nm emission line for boron determination. 230.606 nm was selected for indium determination. Boron/indium signal intensity ratios were used for results. The operating conditions for ICP-OES were as follows:

Table 2. 2 Operating Parameters of ICP-OES

Parameters	Optimum Value
Power, kW	1.2
Frequency, MHz	40.68
Coolant Gas Flow Rate, L/min	19
Auxiliary Gas Flow Rate, L/min	0.5
Nebulizer Pressure, psi	35
Sample Flow Rate, mL/min	0.5

2.2. Boron Determination in Blood Samples

2.2.1. Reagents and Samples

As a stock solution, 1000 mg/L boron solution prepared from boric acid (Merck) in 1.0% (v/v) HNO_3 was used. Standard solutions were prepared in 1.0 M distilled HNO_3 by diluting the stock solution with deionized water from Millipore Milli-Q Water Purification System. The analytical grade 65% (w/w) HNO_3 (Merck) was distilled by the Berghof Acid Distillation System. Boron concentrations of the calibration standards for blood analysis were 5.0, 10.0, 20.0, 50.0 and 100.0 ng/mL.

Blood samples were collected from the same human subjects who gave urine samples in Bandırma region. Like urine samples, blood samples were stored in deep-freeze before analysis.

Stock solution of 100 mg/L Beryllium (Be) (Plasma Pure) in 2.0% (v/v) HNO_3 was used as the internal standard and necessary dilutions were done. Concentration of Be in all standard solutions and samples was adjusted to 25.0 ng/mL. Apart from 25.0 ng/mL Be as internal standard, 1.0% (w/v) sugar was added into calibration standards. The aim was to match the carbon content of the blood and the standards.

Accuracy of the method was checked by using BCR Human Hair as a certified reference material.

2.2.2. Apparatus and Materials

Similar to preparation of urine samples, same micropipettes, PP, PTFE and PE vessels were used during the preparation of standard solutions and samples. In addition, similar cleaning procedures were applied for labware.

2.2.3. Microwave Digestion System

Milestone Ethos PLUS microwave dissolution system was used for digestion of the blood samples. 1.0 mL of the blood sample, which is approximately 1.0 g, was accurately weighed and transferred to the PTFE digestion vessel; a mixture of 2.0 mL concentrated distilled HNO_3 and 2.0 mL concentrated H_2O_2 was added. The digestion vessel was closed and the microwave oven temperature program was applied as seen in Table 2.3.

Table 2. 3 Microwave Digestion Program for blood samples

Time	Temperature
5 min	20 ^{o}C → 100 ^{o}C
5 min	100 ^{o}C
5 min	100 ^{o}C → 150 ^{o}C
5 min	150 ^{o}C

At the end of the digestion process, the PTFE vessels were cooled to room temperature and opened. All the digested solution in the PTFE vessel was transferred

into a PE vessel with a capacity of 15.0 mL; 150 µL of 1000 ng/mL Be solution were added so that final concentration of Be in the solution was 25.0 ng/mL. The test solution was completed to a total mass of approximately 6.0 g using deionized water on balance.

2.2.4. Inductively Coupled Plasma Mass Spectrometer

For this study, Thermo X2 Series Inductively Coupled Plasma Mass Spectrometer was used. Flow injection system was used for sample introduction due to less sample volume. Loop volume was 500 µL. Sampler and skimmer cones of the instrument are made of Nickel.

Boron determination was done by evaluating both ^{11}B and ^{10}B. Internal standard, Be, has one isotope at mass number 9 with 100% abundance. As a result, boron to beryllium ratio was calculated. The operating conditions for ICP-MS were as follows:

Table 2. 4 Operating Parameters of ICP-MS

Parameters	Optimum Value
Extraction Lens Voltage, V	-208
Lens 1 Voltage, V	-3.2
Lens 2 Voltage, V	-63.5
Focus Lens Voltage, V	17.1
1. Diffraction Aperture Voltage, V	-54.9
2. Diffraction Aperture Voltage, V	-207
Quadrupole Voltage, V	-2.5
Hexapole Voltage , V	1.9
Argon Flow Rate in Nebulizer, L/min	0.76
Lens 3 Voltage, V	-188.2
Horizontal Position of Torch	58
Vertical Position of Torch	659
3. Diffraction Aperture Voltage, V	-74.5
Argon Flow Rate to Cool Torch, L/min	18.0
Argon Flow Rate to Produce Plasma, L/min	0.86
Sampling Depth	13
Forward Power, Watt	1400

2.2.5. Total Organic Carbon Analyzer

Shimadzu TOC-V CPH total organic carbon analyzer, at Chemical Engineering Department, METU, was used to determine the carbon contents of the undigested and digested blood samples.

Calibration standards were prepared by using potassium hydrogen phthalate, $KHC_8H_4O_4$ stock solution that includes 1000 mg/L C. Carbon concentrations of the calibration standards were 100, 250, 500 and 1000 mg/L for this study.

CHAPTER 3

RESULTS AND DISCUSSION

For this study, the developed method by our research group was applied with minor changes for boron determination in urine samples and a new analytical method was developed for the determination of boron in blood samples.

3.1. Determination of Boron in Urine Samples by ICP-OES

3.1.1. Optimization of ICP-OES Parameters

For boron determination in urine samples, a method was developed by our research group [72]. Before analyzing the urine samples, repeatability and reproducibility of the system was checked. During initial trials, system did not give repeatable results. Thus, robustness test was applied to obtain optimum values for which system was not affected by conditions such as plasma temperature. Optimization parameters which are power, flow rate of auxiliary and coolant argon, nebulizer pressure and also suction rate of the pump were optimized to get a robust system. Intensity ratios of the Mg II to Mg I should be close to 4.0 or larger for a robust system for axial viewing. Since higher power provides the system to be more robust, powers of 1.3 kW and 1.4 kW were tried with corresponding optimizations. So, two separate optimizations of parameters were done for powers of 1.3 kW and 1.4 kW.

3.1.1.1. Optimization of Flow Rate of Coolant Argon

By keeping the other parameters constant, flow rate of the coolant argon was varied from 16.0 L/min to 18.0 L/min. Intensity ratios of Mg II to Mg I were calculated for each flow rate. Optimization of this parameter was done for both powers of 1.3 kW and 1.4 kW. As it is seen from Figure 3.1, increasing flow rate caused a decrease in the Mg II/ Mg I. Consequently, 16.0 L/min was selected as the coolant flow rate. On the other hand, with a very little difference, 17.0 L/min for flow rate was chosen when power was adjusted to 1.3 kW.

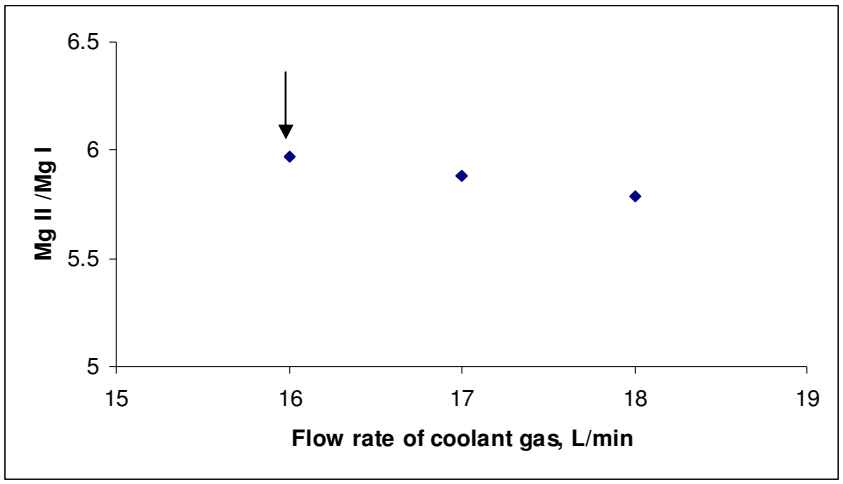

Figure 3. 1 Optimization of the coolant flow rate using the power of 1.4 kW

Flow rate of auxiliary gas: 0.5 L/min, nebulizer pressure: 35.0 psi, sample solution flow rate: 0.5 mL/min

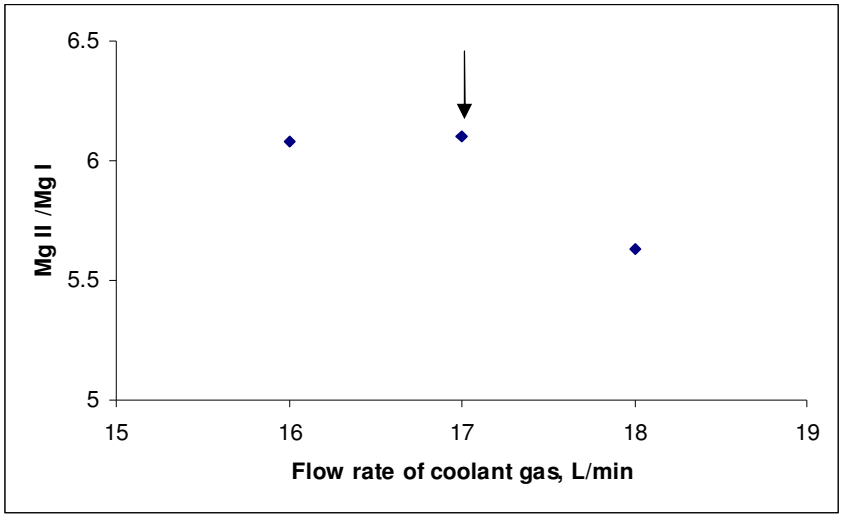

Figure 3. 2 Optimization of the coolant flow rate using the power of 1.3 kW

Flow rate of auxiliary gas: 0.5 L/min, nebulizer pressure: 35.0 psi, sample solution flow rate: 0.5 mL/min

3.1.1.2. Optimization of Nebulizer Pressure

After optimizing the coolant flow rate, pressure of the nebulizer was adjusted. Pressure was varied between 34.0 psi (*pound per square inch*) and 39.0 psi. Again, intensity ratios of the Mg II to Mg I were calculated for both powers of 1.3 kW and 1.4 kW. Results of nebulizer pressure optimization for powers of 1.4 kW and 1.3 kW are shown in Figures 3.3 and 3.4, respectively.

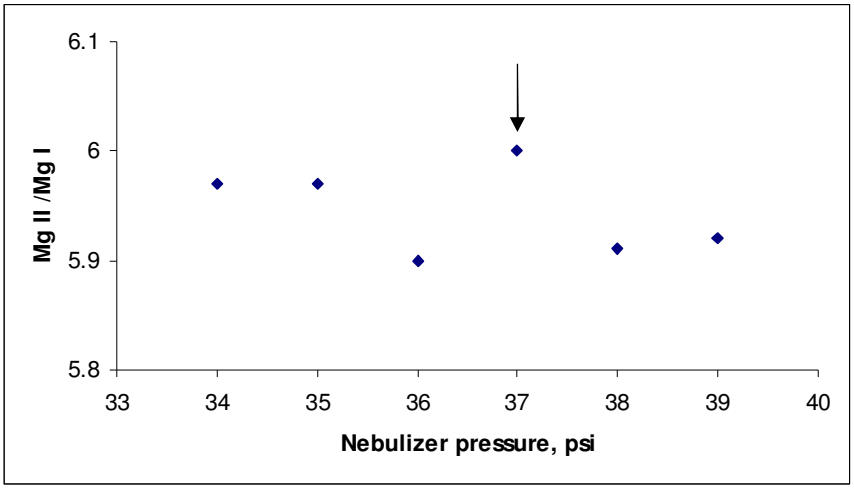

Figure 3. 3 Optimization of the nebulizer pressure using the power of 1.4 kW

Flow rate of auxiliary gas: 0.5 L/min, coolant gas flow rate: 16.0 L/min, sample solution flow rate: 0.5 mL/min

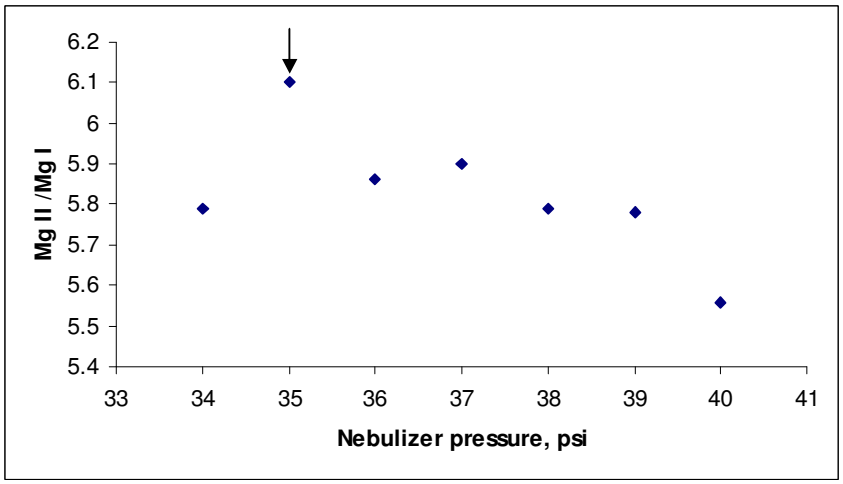

Figure 3. 4 Optimization of the nebulizer pressure using the power of 1.3 kW

Flow rate of auxiliary gas: 0.5 L/min, coolant gas flow rate: 17.0 L/min, sample solution flow rate: 0.5 mL/min

As it is seen from the Figures above, 37.0 psi was chosen as an optimum pressure of nebulizer when power was 1.4 kW while 35.0 psi gave the maximum ratio when applied power was 1.3 kW.

3.1.1.3. Optimization of Sample Solution Flow Rate

Instead of optimizing the internal diameter of the injector as it is stated in some studies [70], suction rate of the pump was optimized. Since the critical point is to reduce the flow of the sample solution, this is easily accomplished by varying the suction rate of the pump. Therefore, pump rate was varied from 0.5 to 1.1 mL/min. 0.6 mL/min was selected as the optimum for power of 1.4 kW as it is seen in the Figure 3.5 whereas 0.5 mL/min was the optimum rate for power of 1.3 kW.

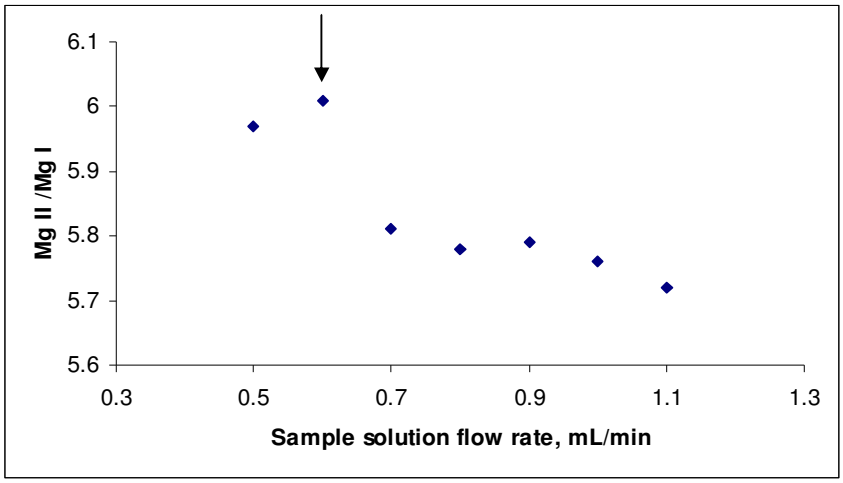

Figure 3. 5 Optimization of sample solution flow rate

Nebulizer pressure: 37.0 psi, coolant gas flow rate: 16.0 L/min, flow rate of auxiliary gas: 0.5 L/min, power: 1.4 kW

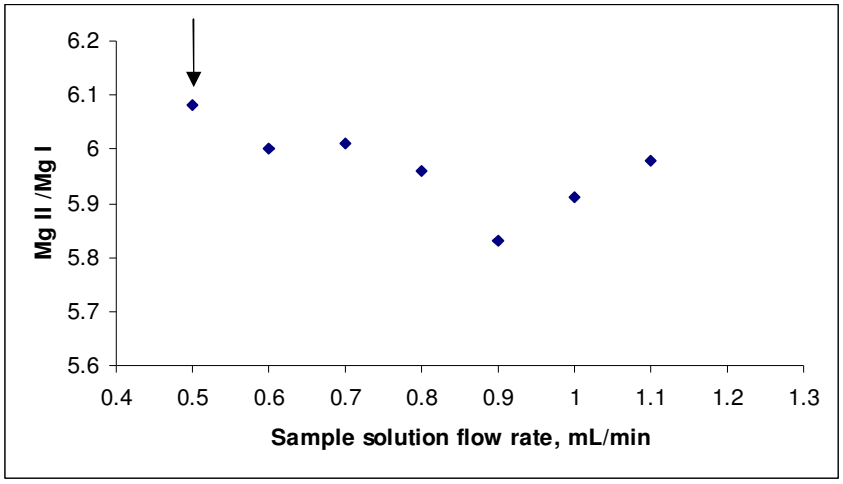

Figure 3. 6 Optimization of sample solution flow rate

Nebulizer pressure: 35.0 psi, coolant gas flow rate: 17.0 L/min, flow rate of auxiliary gas: 0.5 L/min, power: 1.3 kW

3.1.1.4. Optimization of the Flow Rate of Auxiliary Argon

Last parameter to be optimized was the auxiliary argon flow rate. Values were varied between 0.3 L/ min and 0.6 L/min. For both powers, 0.5 L/min auxiliary flow rate gave the highest Mg II/ Mg I ratio. The data are given in Figures 3.7 and 3.8.

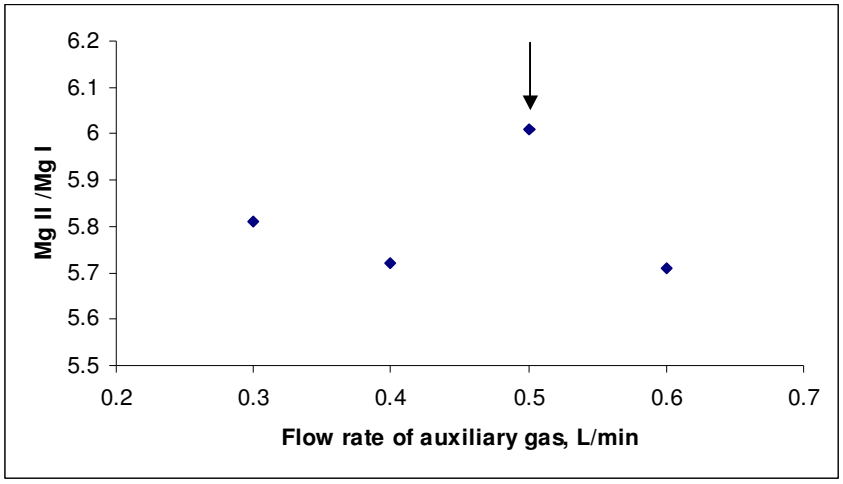

Figure 3. 7 Optimization of the auxiliary gas flow rate using the power of 1.4 kW Nebulizer pressure: 37.0 psi, coolant gas flow rate: 16.0 L/min, sample solution flow rate: 0.6 mL/min

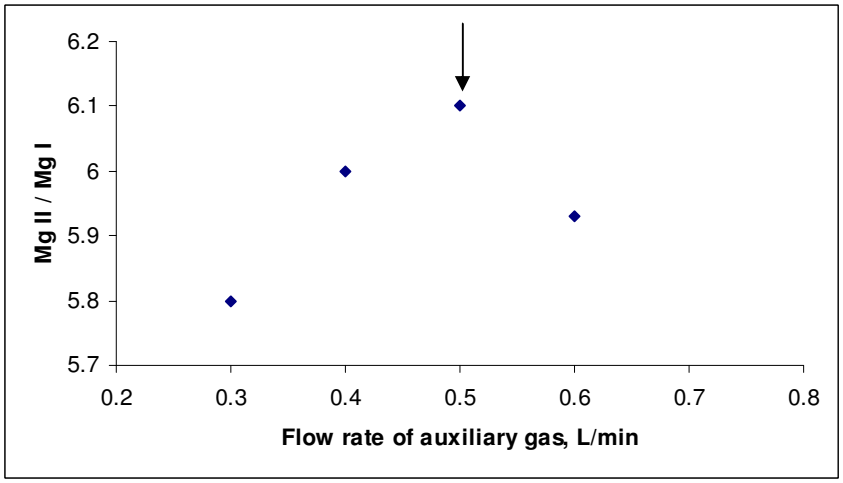

Figure 3. 8 Optimization of the auxiliary flow rate using the power of 1.3 kW Nebulizer pressure: 35.0 psi, coolant gas flow rate: 17.0 L/min, sample solution flow rate: 0.5 mL/min

Since high power and long residence time of analyte in plasma are required for a more robust system, values of the second set were selected as the optimum. Although

power was not suitable, nebulizer pressure and suction rate of the pump were smaller providing long residence time for the sample atoms in plasma.

After optimizations using aqueous B solutions, it was observed that Ar plasma went off in a short time when urine samples were introduced. The reasons were believed to be insufficient coolant argon flow rate and applied power which was relatively high for our instrument. Coolant argon flow rate was not sufficient for this analysis since urine matrix was very dense. Therefore, coolant argon flow rate and power were varied from 17.0 L/min to 19.0 L/min and from 1.3 kW to 1.2 kW, respectively. These values were used during the urine analysis. The final set of parameters for urine analysis is given in in Table 3.1.

Table 3. 1 Optimized parameters for Ar plasma

	Set I	**Set II**	**For Urine Analysis**
Power, kW	1.4	1.3	1.2
Coolant Ar, L/min	16.0	17.0	19.0
Nebulizer pressure, psi	37.0	35.0	35.0
Sample flow rate, L/min	0.6	0.5	0.5
Auxiliary Ar, L/min	0.5	0.5	0.5

3.1.2. Interference Effect of Fe on B Signals

According to literature [6], if the iron concentration of the sample is high, it may interfere to the signals of B. Fe signal at 249.782 nm interferes with B signal at 249.773 nm. It was observed that iron concentration of 5.0 g/L in the sample does not interfere with the boron signal at 249.773 nm [73]. In order to control the possible Fe interference, Fe concentrations of the three different urine samples with

their duplicates were determined. 239.562 nm emission line of Fe was selected due to its high S/N ratio; using this line Fe concentration range of the urine samples was found to be in the range of 0.06 to 0.40 mg/L. Since results were significantly lower than 5.0 g/L, Fe interference to the signals of B was not likely.

3.1.3. Calibration Plot and Signals for Urine Analysis

Calibration standards with concentrations of 0.10, 0.25, 0.50, 1.0 and 2.0 mg/L were used for plotting the calibration graph as shown in Figure 3.9. Each calibration standard included 10.0 mg/L indium internal standard. Concentration of In was chosen big enough to get clear signals.

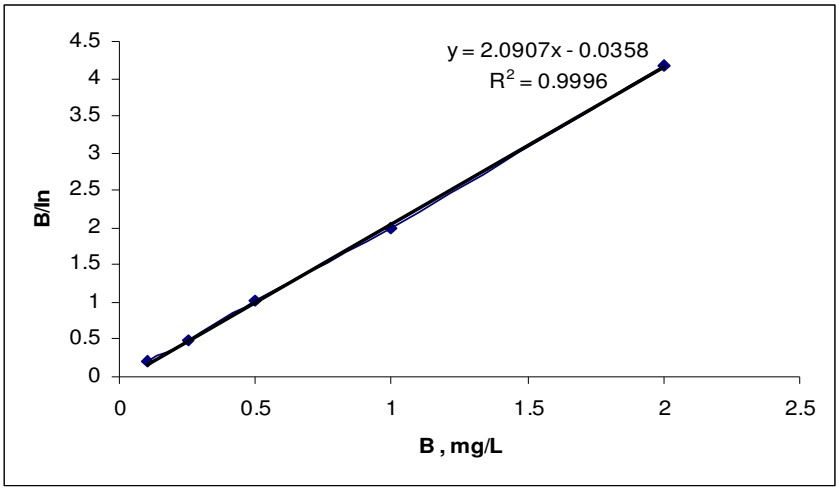

Figure 3. 9 Calibration plot for B by ICP-OES, using conditions in Table 3.1 for urine analysis

Determination of boron was done by selecting the 249.773 nm line of B at which the highest signal to noise ratio was obtained. The wavelength for In was 230.606 nm. Signals of B and Indium are shown in Figures 3.10 and 3.11, respectively.

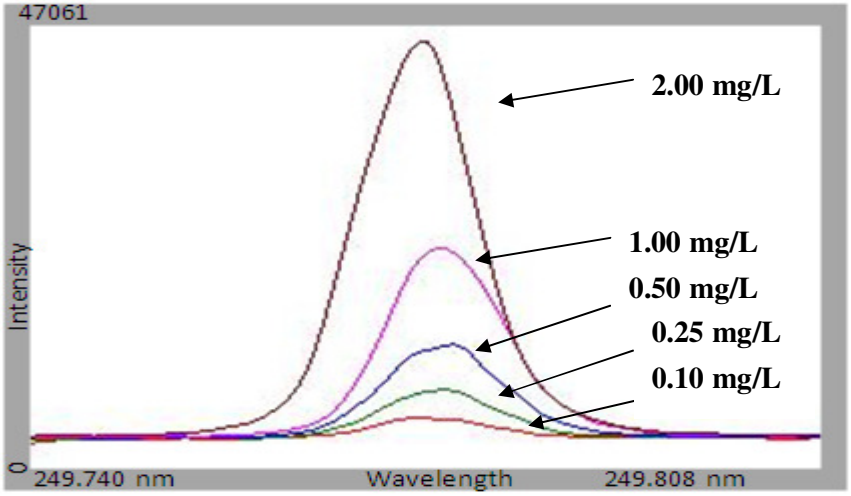

Figure 3. 10 Signals of B by ICP-OES

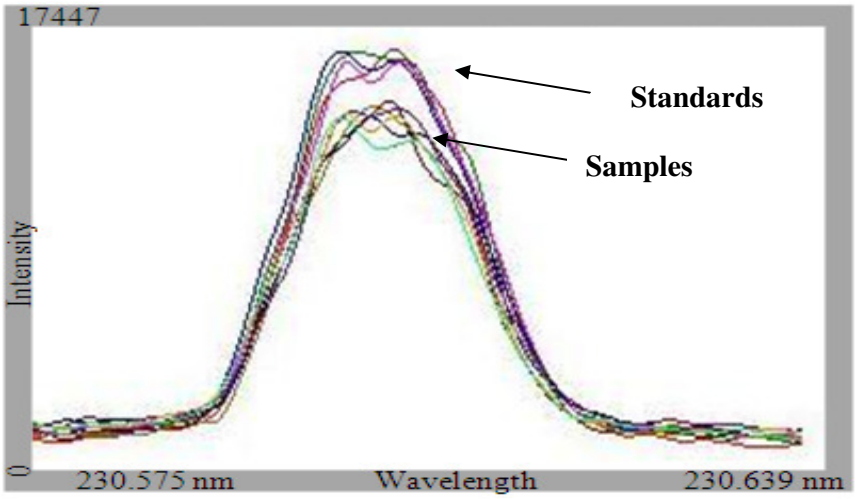

Figure 3. 11 Signals of In by ICP-OES

As it is seen from the Figure 3.11, Indium signals were suppressed in the urine samples because of the matrix effect.

Urine samples were digested and analyzed in duplicate. The signals of the standards and samples with their duplicates are given in Figure 3.12.

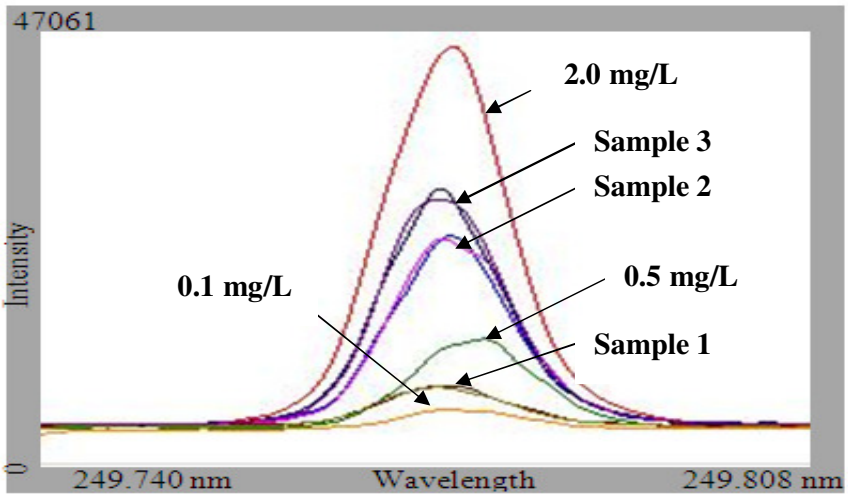

Figure 3. 12 Signals of some standards and samples in duplicate

Standard additions technique was applied for urine samples to check the matrix effect. Boron standard solutions were added into the urine samples to obtain final spike concentrations of 0.25, 0.50 and 1.0 mg/L. Indium internal standard was also spiked to each sample with a final concentration of 10.0 mg/L. Standard addition and direct calibration plots are compared in Figure 3.13. As it is seen slopes of the two graphs are close to each other. Therefore, it was decided that standard addition technique was not necessary; analysis were continued using direct calibration.

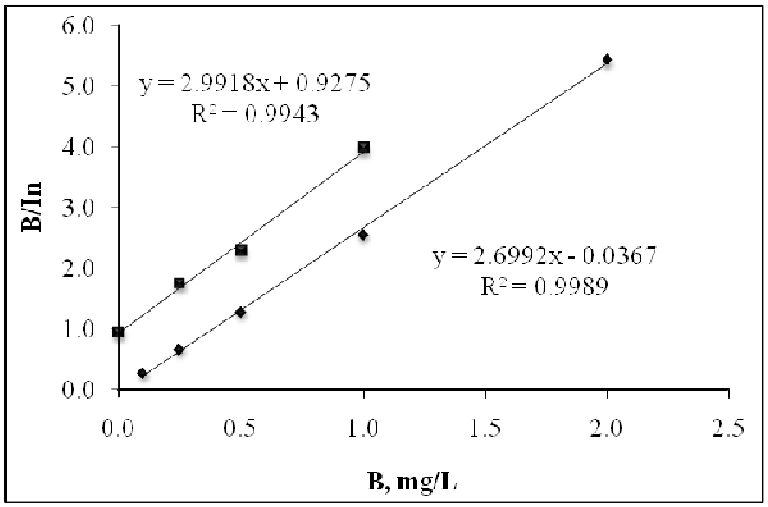

Figure 3. 13 Comparison of the standard addition and direct calibration techniques

For this method, LOD (3s/m) and LOQ (10s/m) were calculated by measuring the lowest concentrated calibration standard five times. Values of LOD, LOQ and linear range are listed in Table 3.2.

Table 3. 2 Analytical Figures of Merit for B with ICP-OES

	B
LOD , mg/L	0.021
LOQ, mg/L	0.070
Linear range, mg/L	0.10 - 5.0

3.1.4. Accuracy Check of the Method

Since there is no suitable standard reference material (SRM) for boron determination in body fluids, accuracy of the method was controlled by using NIST 1573a Tomato Leaves as an SRM. Although matrix of Human Hair CRM is more suitable for urine samples, its B concentration is very low and it is not possible to detect with ICP-OES.

For digestion, 0.50 g of SRM was weighed and digested in microwave oven after addition of 9.5 mL concentrated HNO_3. For microwave digestion, program given in section 2.1.3 was used. Digest was filtered since there was a precipitate. After analysis, B concentration was found to be significantly lower than the certified value. This means some of the B remained in the precipitate. So, 9.0 mL concentrated HNO_3 and 0.5 mL concentrated HF were added to digest 0.50 g of SRM for the next time. The entire solid was dissolved after the addition of HF. In addition, standard addition technique was used to eliminate the suppression effect of calcium. 5.05% (w/w) Ca is found in the SRM used. Plot obtained by using standard addition technique is shown in Figure 3.14. Most concentrated solution was measured 3 times to calculate % RSD. Signals of the same solution increased due to the effect of HF which causes the removal of B from the quartz and borosilicate surfaces of the introduction system. % RSD was calculated as 7.41. Result was found in good agreement with certified value as shown in Table 3.3.

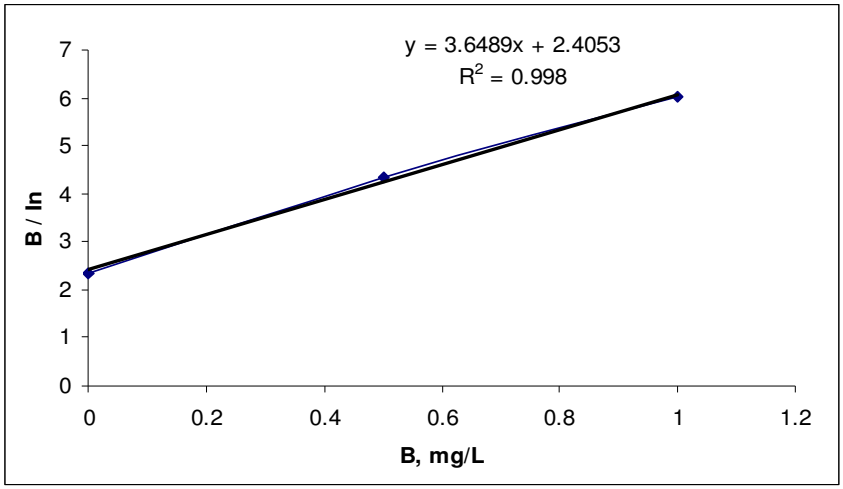

Figure 3. 14 Plot of standard addition technique for B determination in NIST 1573a Tomato Leaves

Table 3. 3 Result of the Accuracy Check for ICP-OES

SRM	Certified, mg/kg	Found, mg/kg
NIST 1573a Tomato Leaves	33.3 ± 0.7	32.9 ± 2.4

3.2. Determination of Boron in Blood Samples by ICP-MS

3.2.1. Method Development with Borosilicate and Quartz Sample Introduction System

At the beginning of the study, memory effect problem which was encountered in literature was checked by using borosilicate and quartz sample introduction system. Spray chamber and nebulizer of this system was made from borosilicate glass while entire torch, including injector tube was made from quartz. For this part of the study, calibration standards of B were prepared in deionized water and introduced to the Ar plasma of ICP-MS. Operating values of it are listed in Table 2.4.

Concentrations of the calibration standards were 5.0, 10.0, 20.0, 50.0 and 100 ng/mL B. Since developed method is to be applied for blood analysis, small sample volume consumption was preferred due to both sample amount limitations and for an easier clean up process. Therefore, a flow injection system was used. Carrier solution was deionized water and a loop volume of 1.0 mL was used. Abundance of ^{11}B is 80.1% while that of ^{10}B is 19.9%. Signals of both boron isotopes were monitored. However, only the signals of ^{11}B were shown in this thesis study because of its higher sensitivity. The calibration plot for ^{11}B is shown in Figure 3.15.

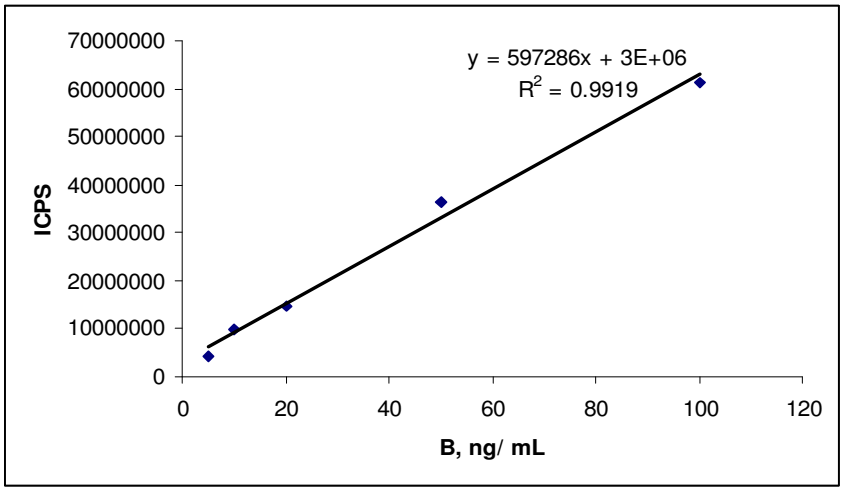

Figure 3. 15 Linear calibration plot for ^{11}B in deionized water

In order to check the memory effect, 10.0 ng/mL B solution was introduced to the system again after the injections of more concentrated B solutions. The signals of 10.0 ng/mL B solution are shown in Figure 3.16. Smallest signal belongs to the 10.0 ng/mL B that was injected at the beginning of the analysis. Other ones belong to the same standard after injection of 500 ng/mL B standard solution. As it is seen, signals were not the same. Largest signal was obtained first after 500 ng/mL B solution. Signals decreased after each injection of the 10.0 ng/mL B solution. This means that memory effect problem is present with this system.

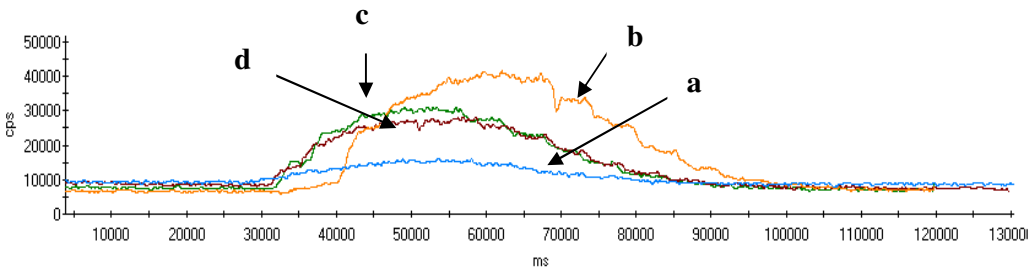

Figure 3. 16 Signals of 10.0 ng/mL ^{11}B standard solution to show memory effect **a)** at the beginning, **b)** after injection of 500 ng/mL B **c)** after the signal obtained in (b) **d)** after the signal obtained in (c)

As suggested by *Sun et al.,* standards were prepared in 0.25% (w/v) mannitol (Duchefa Biochemie) and 0.10 M ammonia (Merck) in order to eliminate memory effect [58]. Mannitol has a chemical formula of $C_6H_{14}O_6$ with an open name hexane-1, 2, 3, 4, 5, 6-hexol. Mixture of 0.25% (w/v) mannitol and 0.10 M ammonia solution was also used as a wash solution after each measurement once. Calibration plot for ^{11}B with these standards is shown in the Figure 3.17.

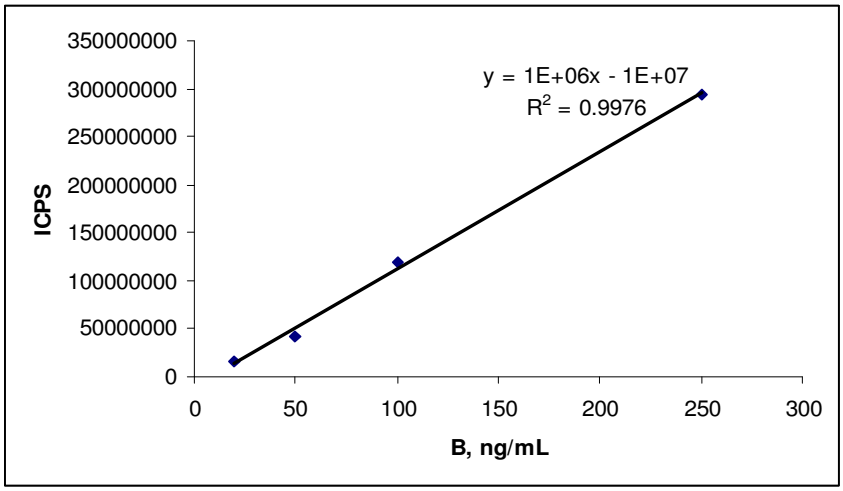

Figure 3. 17 Calibration plot for B prepared in 0.25% (w/v) mannitol and 0.10 M ammonia solution; ^{11}B was measured

Signal shapes were not regular and symmetrical when ammonia and mannitol mixture was added to B standard solutions. Sharp increase at the beginning of the peak resulted from the ammonia and mannitol mixture. Signal obtained by 0.25% (w/v) mannitol and 0.10 M ammonia mixture as a wash solution is shown in Figure 3.18. On the other hand, the signal for 20 ng/mL B in 0.25% (w/v) mannitol and 0.10 M ammonia solution is given in Figure 3.19.

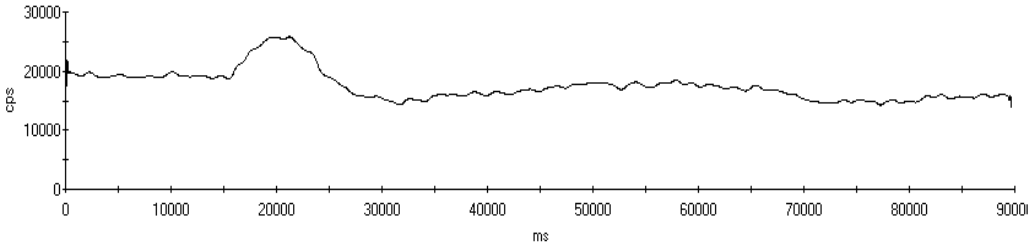

Figure 3. 18 Signal of 0.25% (w/v) mannitol and 0.10 M ammonia solution as a wash solution

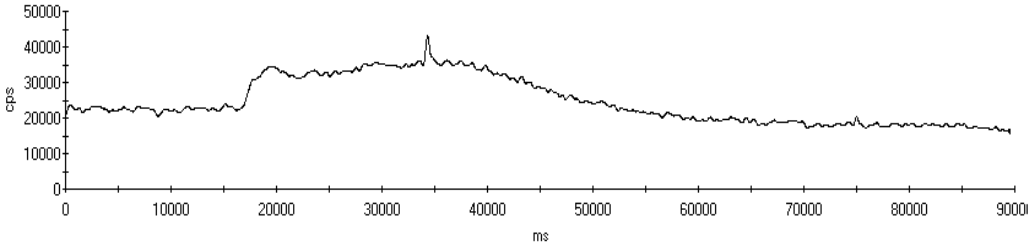

Figure 3. 19 Signal of 20 ng/mL ^{11}B in 0.25% (w/v) mannitol and 0.10 M ammonia solution

The peak which appears between 15-25 seconds after injection corresponds to adsorbed B on sample introduction system from previous measurement for both cases shown in Figure 3.18 and Figure 3.19. Wash solution was injected after each standard solution once.

Plasma instability is a very important parameter that affects the results of ICP-MS analysis. Therefore, in order to make sure that result will not be affected from plasma fluctuations; proper internal standard should be used. Since ions of the both elements are affected from the temperature change in the same time interval and in supposedly a similar manner, their signal ratio will provide a result with an improved precision and accuracy.

Initially, Indium (In) was used as an internal standard. In all standard solutions, In concentration was kept at 25.0 ng/mL. Since concentration of indium in blood is too low, it is a suitable internal standard. The natural abundance of ^{115}In is 95.7% while that of ^{113}In is 4.3%.

When preparing the calibration standards with an In internal standard, 0.25% (w/v) mannitol and 0.1 M ammonia were not added. Instead, standards were prepared in 1.0 M HNO_3. 0.25% (w/v) mannitol and 0.1 M ammonia solution was used only as a wash solution between measurements of standard solutions. Calibration plot for ^{11}B when In was used is shown in Figure 3.20.

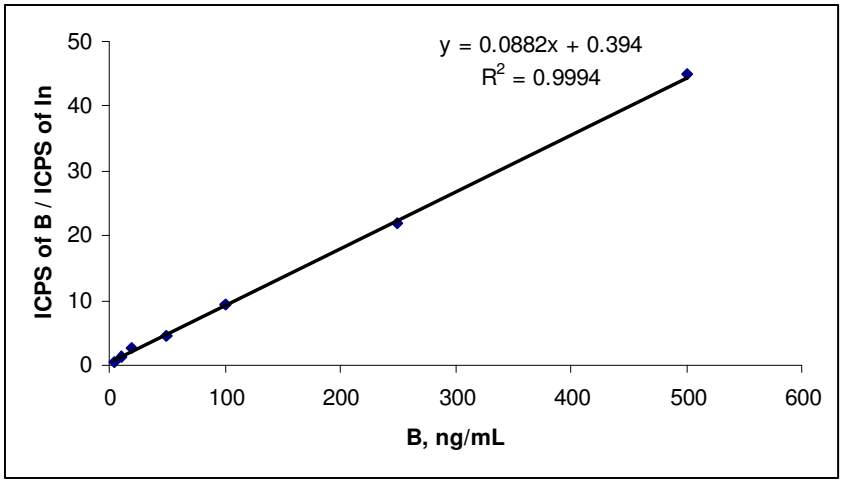

Figure 3. 20 Calibration plot for ^{11}B using Indium as an internal standard in 1.0 M HNO_3

0.25% (w/v) mannitol and 0.10 M ammonia solution which was used after each standard solution eliminates memory effect problem. Signals of the same 10.0 ng/mL of B solution with an Indium internal standard are shown in Figure 3.21. One signal corresponded to the signal of 10.0 ng/mL of B introduced at the beginning of the analysis while the other was obtained after 1000 ng/mL B standard was introduced to the system. Mannitol-ammonia solution was injected after each standard solution. As it is seen clearly, two signals were the same. In conclusion, 0.25% (w/v) mannitol and 0.10 M ammonia solution was very effective for eliminating the memory effect.

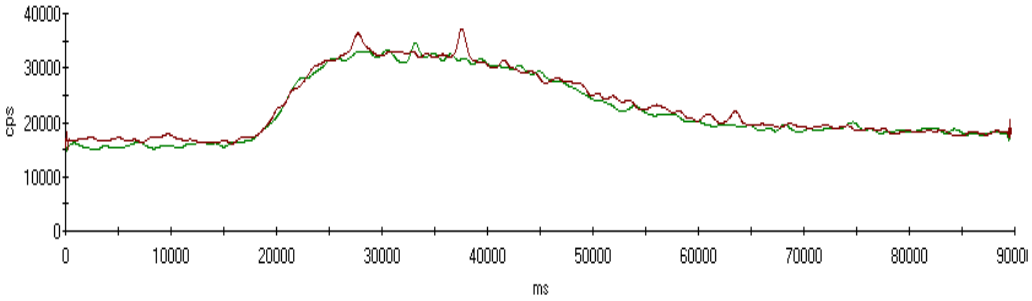

Figure 3. 21 ^{11}B signals of the same 10.0 ng/mL boron standard solution; mannitol-ammonia mixture was used as a wash solution

When more detailed library search was made about internal standard, Beryllium (^{9}Be) was found to be a more suitable internal standard for boron determination by ICP-MS. Since ICP-MS was used for this study, closeness of the masses of the analyte and internal standard is important. Furthermore, Be concentration in blood is very low. Therefore, ^{9}Be was used as an internal standard in the rest of the study. 0.25% (w/v) mannitol and 0.10 M ammonia solution was used once as a wash solution between measurements of standard solutions. The calibration plot for ^{11}B with ^{9}Be internal standard is shown in Figure 3.22.

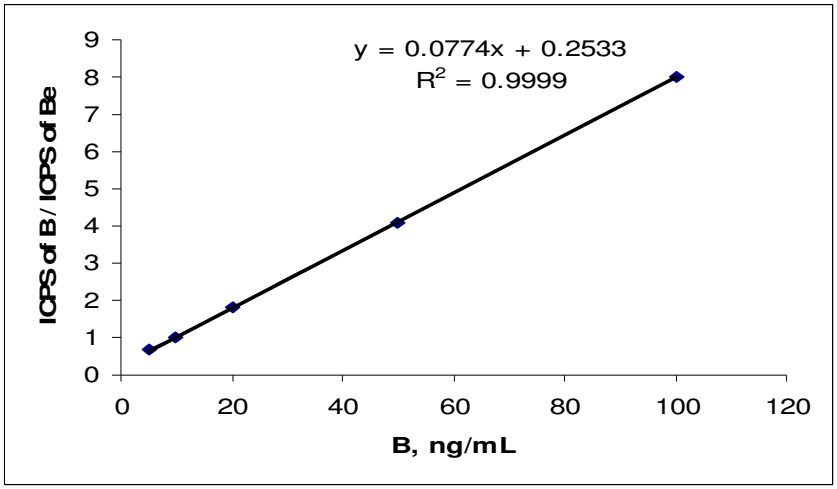

Figure 3. 22 Calibration plot for ^{11}B using ^{9}Be as an internal standard in 1.0 M HNO_3

Concentration of Be in all standard solutions was 25.0 ng/mL.

For this system, LOD (Limit of Detection) and LOQ (Limit of Quantification) were calculated by using the signals of 10.0 ng/mL B standard solution which was measured eight times. LOD and LOQ results are listed in Table 3.4.

Table 3. 4 Analytical Figures of Merit for ^{11}B and ^{10}B with borosilicate and quartz sample introduction system

	^{11}B	**^{10}B**
LOD , ng/mL	1.50	2.97
LOQ, ng/mL	5.00	9.89

In order to compare the sensitivities, calibration graph for ^{10}B was also plotted in Figure 3.23.

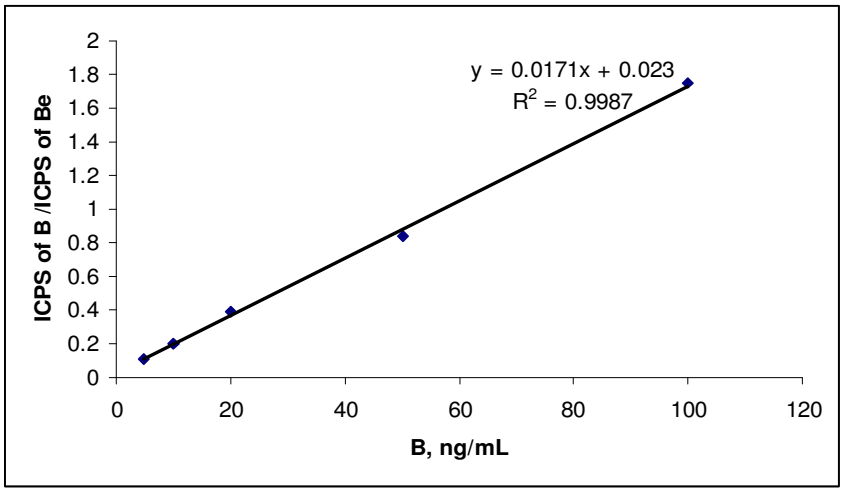

Figure 3. 23 Calibration plot for ^{10}B using ^{9}Be as an internal standard in 1.0 M HNO_3

As it is seen from the slopes, sensitivity of ^{10}B was nearly 4 fold lower than that of ^{11}B. The difference corresponds to the natural abundances of these isotopes. Abundance of ^{11}B is 80.1% while that of ^{10}B is 19.9%. LOD and LOQ were calculated using ^{10}B signals using a standard of 10.0 ng/mL B and eight measurements; results are shown in Table 3.4.

3.2.2. Method Development with PFA-Alumina Sample Introduction System

Although using 0.25% (w/v) mannitol and 0.10 M ammonia solution as a wash solution solved the memory effect problem, washing the system after each B containing solution needs extra time and this may become a significant problem for a large number of analysis. Therefore, new system that includes perfluoroalkoxy (PFA) spray chamber and nebulizer with an alumina injector tube in a quartz torch was used for this study. Since PFA and alumina do not contain B in their structures, memory effect problem for boron should not be expected. PFA spray chamber and

torch with an alumina injector tube used for the rest of the study are shown in Figures 3.24 and 3.25, respectively.

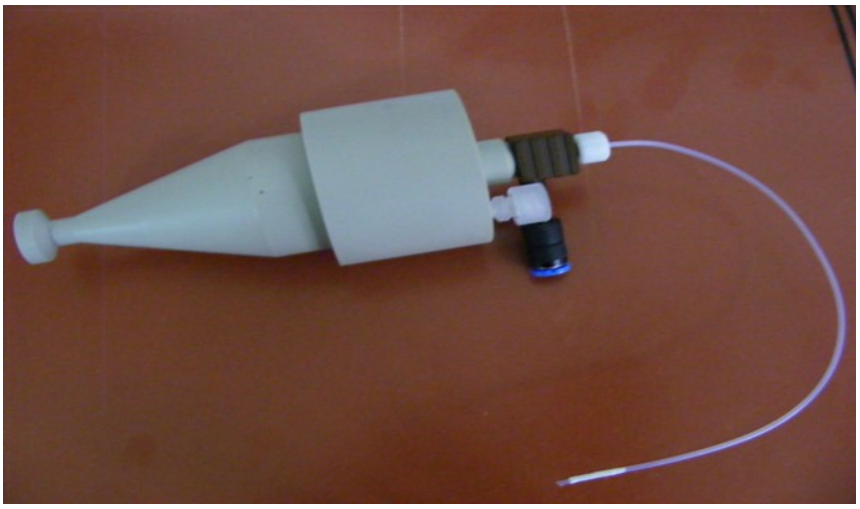

Figure 3. 24 PFA spray chamber used in the study

Figure 3. 25 Quartz torch with an alumina injector tube used in the study

For measurements, standard solutions of 2.0, 5.0, 10.0, 20.0, 50.0 and 100.0 ng/mL B with 25.0 ng/mL Be internal standard were prepared in 1.0 M distilled HNO_3 . Again by using the flow injection system but this time with a 500 µL loop volume, standard solutions were introduced to the system. Each standard solution was measured three times. The calibration plot for B obtained by this new system can be seen in Figure 3.26.

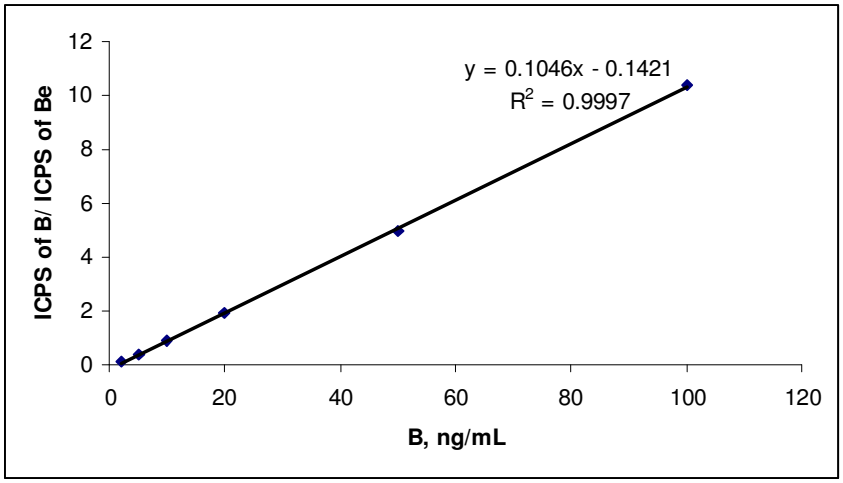

Figure 3. 26 Calibration plot for ^{11}B using ^{9}Be as an internal standard with PFA-Alumina sample introduction system

Signals of the standards are shown in Figure 3.27. These signals belong to 5.0, 10.0, 20.0 and 50.0 ng/mL B standard solutions.

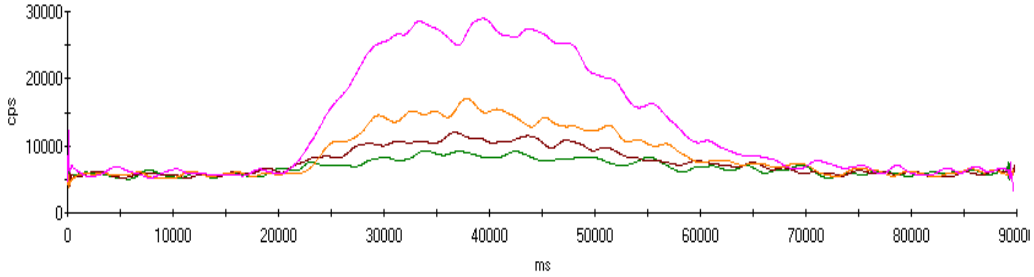

Figure 3. 27 ^{11}B signals of calibration standards with PFA-Alumina sample introduction system

With PFA-Alumina sample introduction system, baseline of the boron signal decreased. When the baseline signals were compared, using the borosilicate system at least 10000 counts were obtained while approximately 5000 counts were obtained by using PFA-Alumina sample introduction system. Baseline signal corresponds to the B concentration of deionized water plus adsorbed B on the introduction system from previous measurement for borosilicate introduction system. Deionized water was the carrier solution for this study.

LOD and LOQ were calculated using the PFA-Alumina sample introduction system; results are listed in Table 3.5. For these calculations, 10.0 ng/mL B standard solution was measured six times.

Table 3. 5 Analytical Figures of Merit for ^{11}B with PFA-Alumina sample introduction system

	^{11}B
LOD, ng/mL	2.17
LOQ, ng/mL	7.24

As it is seen from Table 3.5 LOD and LOQ values of the system were calculated in ng/mL units. However, evaluation of the sample results with respect to LOD and LOQ in same unit is more meaningful so these values were converted to ng/g unit. For calculations, LOD and LOQ values of the system were multiplied by the dilution factor and then divided to sample density which was 1.17 g/mL. LOD and LOQ values of the sample are given in Table 3.6.

Table 3. 6 Analytical Figures of Merit of the sample for ^{11}B with PFA-Alumina sample introduction system

	^{11}B
LOD, ng/g	11.1
LOQ, ng/g	37.1

3.2.2.1. Effect of Be on Signal of ^{10}B

Although ^{11}B signals were used for calibrations, in fact both ^{10}B and ^{11}B signals were recorded during the study. It seemed possible that Be may interfere with the ^{10}B signal by forming BeH^+ with a nominal mass of 10. Therefore, this possibility was evaluated by preparing Be solutions with increasing concentrations. The concentrations of the solutions were 10.0, 20.0, 25.0, 50.0 and 100.0 ng/mL Be.

Contrary to the assumption, increased concentrations of Be did not give any significant signals with a nominal mass of 10. This situation is illustrated in Figure 3.28.

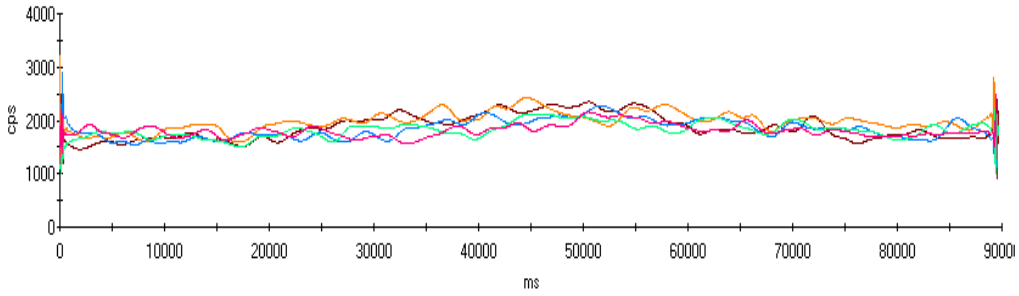

Figure 3. 28 Signals at nominal mass 10, for various concentrations of Be

Therefore, Be can be used as an internal standard and if it is necessary ^{10}B signals can also be used conveniently for boron determination.

3.2.2.2. Solution Composition for Digestion of Blood Samples

Since ICP-MS was used for this study, digestion process of the blood samples was necessary. Otherwise, large amounts of complex-structured proteins and other organic compounds can cause clogging of the nebulizer and sampling cone in addition to matrix effects caused in plasma.

Acid digestion procedure includes one kind of acid or acid mixtures. For the digestion of organic samples, HNO_3 and H_2O_2 mixture is generally used. This mixture provides a strong oxidation. Besides the acid mixture, amounts and ratio of these reagents in the mixture are important.

Since it is known that boron concentration in blood is ng/mL level, dilution above 10-fold is not feasible. Therefore, a mixture of 2.0 mL concentrated distilled HNO_3 and 2.0 mL concentrated H_2O_2 provided a clear solution for approximately 1.0 g

blood samples after microwave digestion with a reasonable dilution. This composition was used for further digestions.

By considering the spiking of Be internal standard solution into the digested blood sample with 4.0 mL acid mixture; blood sample can be diluted 6-fold in minimum. Since there is no volumetric flask in volume of 6.0 mL, sample was diluted to approximately 6.0 g using balance.

3.2.2.3. Effect of Sodium on Signals of B and Be

As it is known, the matrix composition of blood is complicated. It consists of inorganic salts of sodium, potassium, calcium etc. and a high concentration of protein (approximately 70 g/L), together with a variety of trace substances. So, possible effects of Na^+ on the signals of B and Be was studied.

Na^+ ion can suppress the signals of B and Be by space-charge effect. Space-charge effect is observed when sample includes large concentrations of the high-mass matrices. These high-masses defocus the ion beam by pushing the lighter elements out of the way. This effect leads to poor sensitivity and detection limits due to poor transmission of the ions through the ion optics [74]. Na^+ ion with a mass number of 23 is bigger than B^+ and Be^+ ions and is likely to cause space-charge effect.

According to a study by *Yip et al.* the concentration of Na^+ in whole blood is between 135-148 mmol/L [75], corresponding to 3105- 3404 mg/L or 0.3105-0.3404% (w/v) Na. Since blood samples were diluted approximately 6-fold for this study, expected Na^+ concentration in the samples would be approximately 0.05-0.06% (w/v).

In addition to high mass number, concentration of Na in the test samples was high, in mg/L levels. So, space-charge effect of Na^+ is expected on B and Be ions.

In order to control any Na^+ effect, different concentrations of Na_2SO_4 were added to 20.0 ng/mL B solutions which included 25.0 ng/mL Be. Each solution was introduced to the system three times and the average was used for calculations. The percent changes of ^{11}B, ^{10}B and ^{9}Be signals for different Na ion concentrations are shown in Table 3.7.

Table 3. 7 % change of the ^{11}B, ^{10}B and ^{9}Be signals for different Na ion concentrations; N=2

	% change for ^{11}B	**% change for ^{10}B**	**% change for ^{9}Be**
20.0 ng/mL B+25.0 ng/mL Be	**-**	**-**	**-**
0.03% w/v Na+20.0 ng/mL B+25.0 ng/mL Be	- 30.7 ± 2.8	- 30.4 ± 2.7	- 30.6 ± 2.8
0.06% w/v Na+20.0 ng/mL B+25.0 ng/mL Be	- 36.7 ± 3.3	- 32.6 ± 3.0	- 34.3 ± 3.1
0.12% w/v Na+20.0 ng/mL B+25.0 ng/mL Be	- 41.5 ± 3.8	- 41.6 ± 3.8	- 37.0 ± 3.4

As it is seen from the Table 3.7, as the Na ion concentration increases, signals of ^{11}B, ^{10}B and ^{9}Be were suppressed more.

When plasma instability is considered during the analysis, direct comparison of the signals of same element is not suitable and it may not give the correct result. So, ratios of ^{11}B to ^{9}Be and ^{10}B to ^{9}Be were calculated to check Na ion effect. These ratios and their % changes for different Na ion concentrations are listed in Table 3.8.

Table 3. 8 Ratios of ^{11}B to ^{9}Be and ^{10}B to ^{9}Be and also their % changes for different Na ion concentrations; N=2

	$^{11}B/^{9}Be$	**% change for $^{11}B/^{9}Be$**	**$^{10}B/^{9}Be$**	**% change for $^{10}B/^{9}Be$**
20.0 ng/mL B+25.0 ng/mL Be	2.56±0.02		0.52±0.01	
0.03% w/v Na+20.0 ng/mL B+25.0 ng/mL Be	2.55±0.02	**- 0.4±0.1**	0.51±0.01	**- 2.3±0.5**
0.06% w/v Na+20.0 ng/mL B+25.0 ng/mL Be	2.49±0.02	**- 3.0±0.6**	0.50±0.01	**- 3.4±0.7**
0.12% w/v Na+20.0 ng/mL B+25.0 ng/mL Be	2.38±0.02	**- 7.1±1.5**	0.47±0.01	**- 9.5±1.9**

According to results, space charge effect of Na was confirmed. $^{10}B/^{9}Be$ was affected slightly more than $^{11}B/^{9}Be$ in the presence of Na^{+} as shown in Table 3.8. Therefore, using the ratio of ^{11}B to ^{9}Be was more reliable and this result also confirmed the benefits obtained by using ^{9}Be as an internal standard. Furthermore, in the test solution of blood, Na ion concentration was between 0.05- 0.06% (w/v). Percent change for $^{11}B/^{9}Be$ was -3.0 when Na^{+} concentration was 0.06% (w/v). An error up to 5.0% can be tolerated for this kind of analyses. It has been demonstrated that the use of internal standard minimizes the errors that can be caused by the presence of Na in blood samples.

Concentrations of three important ions found in blood in large quantities are listed in Table 3.9 [76]. As it is seen, concentrations of K^{+} and Ca^{2+} ions in blood are much lower than Na^{+} ion. So, possible effects of these ions on B and Be signals were not studied.

Table 3. 9 Concentrations of important ions in blood

Ion	Concentration in whole blood, mM
Na^+	135-148
K^+	3.5-4.5
Ca^{2+}	$(4.5\text{-}5.5) \times 10^{-6}$

3.2.2.4. Effect of Carbon on Signals of B and Be

When conventially low resolution mode of the ICP-MS is considered; spectral interference of ^{12}C on ^{11}B is possible. Furthermore, C could increase the B and Be signals by charge-transfer reaction. Charge transfer reaction is a chemical ionization process and occurs when hard to ionize elements have ionization potentials lower than carbon (11.36 eV) in the presence of it [77]. B and Be are only 58% and 75% ionized in the plasma, respectively [65]. Charge transfer reaction occurs between positively charged carbon species and B (8.3 eV) and Be (9.3 eV) in the central channel of the plasma discharge:

$$C^+ \text{ species} + M \rightarrow M^+ + C \text{ species}$$

This reaction is not valid for the elements with ionization energies much lower than carbon since their ionization efficiencies are close to 100% in normal ICP-MS conditions [77]. First ionization potentials of some elements are listed in Table 3.10.

Table 3. 10 First ionization potentials of some elements

Element	Ionization Potential, eV	Element	Ionization Potential, eV
B	8.29	**Ca**	6.11
Be	9.32	**In**	5.79
C	11.36	**Rh**	7.46
Na	5.14	**Cl**	12.97
K	4.34	**Fe**	7.87

In order to check these effects, sugar ($C_6H_{12}O_6$) was added to B standard solutions as a carbon source. Sugar contents of the solutions were varied from 0.5% (w/v) to 2.0% (w/v). In terms of mg/L; carbon concentrations range from 2000 to 8000. All standard solutions included 20.0 ng/mL B and 25.0 ng/mL Be. Apart from ^{11}B, the tail of the ^{12}C signal might also interfere with ^{10}B and ^{9}Be signals. So, in addition to the signal of ^{11}B, effects of C on these signals were controlled. ICPS of ^{11}B, ^{10}B and ^{9}Be are given in Table 3.11 with increasing sugar contents.

Table 3. 11 ICPS of ^{11}B, ^{10}B and ^{9}Be with increasing sugar contents

	ICPS of ^{11}B	**ICPS of ^{10}B**	**ICPS of ^{9}Be**
20.0 ng/mL B+25.0 ng/mL Be	4651330	1312694	2206807
0.5% w/v sugar +20.0 ng/mL B+25.0 ng/mL Be (0.20% w/v C)	5896970	1449478	2244469
1.0% w/v sugar +20.0 ng/mL B+25.0 ng/mL Be (0.40% w/v C)	6196523	1502661	2281329
1.5% w/v sugar +20.0 ng/mL B+25.0 ng/mL Be (0.60% w/v C)	6849674	1545118	2317447
2.0% w/v sugar +20.0 ng/mL B+25.0 ng/mL Be (0.80% w/v C)	7406586	1686090	2470419

From Table 3.11, it was concluded that presence of C in the solutions increased the signals of ^{11}B, ^{10}B and ^{9}Be. In order to evaluate how much they were increased, percent change of each was calculated with increasing sugar content. Percent change of the ^{11}B, ^{10}B and ^{9}Be signals for different sugar contents are listed in Table 3.12.

Table 3. 12 % change of the ^{11}B, ^{10}B and ^{9}Be signals for different sugar contents; N=2

	% change for ^{11}B	**% change for ^{10}B**	**% change for ^{9}Be**
20.0 ng/mL B+25.0 ng/mL Be	**-**	**-**	**-**
0.5% w/v sugar +20.0 ng/mL B+25.0 ng/mL Be (0.20% w/v C)	26.8±1.6	10.4±0.6	1.7±0.1
1.0% w/v sugar +20.0 ng/mL B+25.0 ng/mL Be (0.40% w/v C)	33.2±2.0	14.5±0.8	3.4±0.1
1.5% w/v sugar +20.0 ng/mL B+25.0 ng/mL Be (0.60% w/v C)	47.3±2.9	17.7±1.0	5.0±0.1
2.0% w/v sugar +20.0 ng/mL B+25.0 ng/mL Be (0.80% w/v C)	59.2±3.6	28.4±1.7	11.9±0.2

When % changes were calculated, it was easily seen that Be signal were affected the least from the presence of C. In addition, % change of ^{10}B signals were less than that of ^{11}B signals. However, by considering the plasma instability, ratios of the B to Be signals should be calculated to evaluate the effects clearly. Ratios and their % changes with increasing sugar content are listed in Table 3.13.

Table 3. 13 Ratios of ^{11}B to ^{9}Be and ^{10}B to ^{9}Be and also their % changes with increasing sugar contents; N=2

	$^{11}B/^{9}Be$	**% change for $^{11}B/^{9}Be$**	**$^{10}B/^{9}Be$**	**% change for $^{10}B/^{9}Be$**
20.0 ng/mL B+25.0 ng/mL Be	2.11±0.13		0.58±0.03	
0.5% w/v sugar +20.0 ng/mL B+25.0 ng/mL Be (0.20% w/v C)	2.63±0.16	**24.5±1.7**	0.64±0.04	**9.5±0.7**
1.0% w/v sugar +20.0 ng/mL B+25.0 ng/mL Be (0.40% w/v C)	2.72±0.17	**28.7±2.0**	0.66±0.04	**11.6±0.9**
1.5% w/v sugar +20.0 ng/mL B+25.0 ng/mL Be (0.60% w/v C)	2.96±0.18	**40.1±2.8**	0.67±0.04	**13.0±1.0**
2.0% w/v sugar +20.0 ng/mL B+25.0 ng/mL Be (0.80% w/v C)	3.00±0.18	**42.1±2.9**	0.68±0.04	**15.7±1.2**

As it is expected, % change for $^{11}B/^{9}Be$ was bigger than that for $^{10}B/^{9}Be$ since ^{11}B signal was affected most from the carbon. According to literature [65], charge transfer effect increases the signal of B more than Be by enhancing the degree of ionization which is less for B (58%) as compared with ^{9}Be (75%) in the normal plasma conditions. Therefore, reason for the biggest increase on the ^{11}B signal can be explained by combined effects of both spectral and charge transfer mechanism. Charge transfer effect should cause the same enhancement for both ^{11}B and ^{10}B. However, spectral effect for ^{11}B is higher. Therefore, the difference between % change values for $^{11}B/^{9}Be$ and $^{10}B/^{9}Be$ is due to spectral effect. Furthermore, the values of $^{11}B/^{10}B$ ratio at different C concentrations gave information about interferences. If there is no change, charge transfer effect is present. However, in case of spectral interference the ratio should increase.

Since blood contains an appreciable organic content, a high carbon concentration is present. From the tables above and explanations, it was certain that C concentration of 2000 mg/L and more affected the B and Be signals and also B/Be ratios. Therefore, it was very important to know the C content of the digested blood to match the C matrix of the standards and samples for reliable results.

Carbon contents of the undigested and digested blood were measured by total organic carbon analyzer. After 100-fold dilution with 0.14 M HNO_3, undigested blood sample was analyzed. Digested blood was diluted 100-fold in total, too. Deionized water was used for dilution after acid digestion. The calibration plot for C standards is given in Figure 3.29.

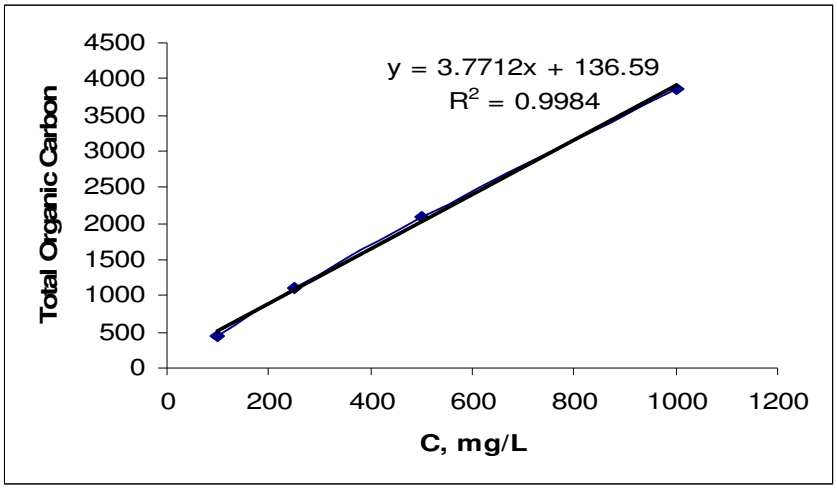

Figure 3. 29 Calibration plot for C standards

C contents of the six different undigested bloods ranged from 94000 to 112500 mg/L. This value corresponds to 9-11% (w/v). On the other hand, when digested; C contents of the same blood samples were reduced to 1.4 - 4.3% (w/v), mostly approximately 2.0% (w/v). When average of these six digested blood samples were calculated 2.4% (w/v) was obtained for carbon content.

In addition to total organic carbon content, inorganic carbon contents of both digested and undigested bloods were measured. Approximately 50.0 mg/L inorganic C was measured in undigested blood whereas 275.0-362.5 mg/L inorganic C was calculated for digested blood. These values are much lower as compared with organic content.

In conclusion, it was obvious that C content of the digested blood was still significantly high to affect the signals for analysis. When 6-fold dilution of the digested blood was considered, (2.4/6) 0.4% (w/v) C was present in the final solution. From calculations by using the molecular weight of sugar (180 g/mol) and carbon (72 g/mol), C content of the final solution was found to be similar to a solution with 1.0% (w/v) sugar. Unfortunately, carbon in the solutions did not affect the signals of ^{11}B and ^{9}Be similarly. Since $^{11}B/^{9}Be$ ratio was used for the calculations of the boron concentrations in blood, this difference could cause wrong results if standards did not include same concentration of carbon. That's why 1.0% (w/v) sugar was added into calibration standards to match the carbon content and eliminate this difference.

Apart from affecting the B and Be signals, C which is present in the blood samples caused deposition on the cones and deformed the orifices of the sampler and skimmer cone. The photos of sampler and skimmer cone with and without C deposition to show the difference are shown in Figures 3.30 and 3.31, respectively.

Figure 3. 30 Skimmer cones with (a) and without (b) C deposition

Deposited carbon can be seen easily from the photo. New skimmer cone was located on the right-side.

Figure 3. 31 Sampler cones with (a) and without (b) C deposition

Cones were cleaned or replaced with new ones after approximately 100 measurements. Sensitivity of the system decreases as deposition increases.

After all, elimination of C from the blood samples was needed in order to extend the life time of the cones and obtain more reliable results. For carbon elimination, vaporization of the digested samples was tested. This process was performed on hot-plate using PTFE vessels. Temperature of the hot-plate was adjusted to 200 ^{o}C. When sample was vaporized to the half volume, its C content was reduced to half. However, vaporization was not a proper way to eliminate carbon. During vaporization on hot-plate at 200 ^{o}C boron might also volatilize from the solution. So, open-digestion process was applied to three parallels of blood sample and its C concentration was compared with the same blood sample digested by microwave.

For open-digestion of blood samples, glass tubes with a long, narrow neck were used; heating was accomplished using an Al-block heater where temperature was controlled by a thermocouple system. Since only C concentration was important for this part, usage of glass was not a problem. 2.0 mL of concentrated HNO_3 were added onto 1.0 mL of blood and temperature was increased stepwise to 70 ^{o}C, 85 ^{o}C and 95 ^{o}C and kept at 95 ^{o}C until samples turn into clear light brown color. After sufficient cooling, 2.0 mL of concentrated H_2O_2 were added at 35 ^{o}C and again, temperature was increased stepwise to 95 ^{o}C. Digestion process was ended when gas evolution stopped [78]. By open-digestion process C concentration in that blood sample was calculated as 1.3% (w/v) while it was 3.6% (w/v) when using microwave for digestion. Therefore, open-digestion was more effective for C removal but PTFE tubes were needed to check whether B was also volatilized or not during the open-digestion.

In addition to open-digestion, microwave digested samples were radiated with UV radiation to remove carbon. UV lamp with a 254 nm was used and parallel samples were radiated 3 and 6 hours, respectively. According to results, UV radiation helped to reduce C concentration 38% when samples were exposed to UV radiation for 3

hours. However, exposure for 6 hours did not increase the C elimination more. More detailed study can be performed to minimize the C content as much as possible.
Although both open digestion and UV irradiation were found to be useful for reducing carbon content, for a large number of analyses these procedures are not practicable. Therefore, these approaches were not used furthermore.

3.2.2.5. Accuracy Check of the Method

After developing the method, its accuracy was checked. Unfortunately, present standard reference materials of whole blood do not have any certified value for boron. Hence, the BCR Human Hair certified reference material was used for the accuracy check. It should be stated that B concentration for this reference material is given as informative value. Developed digestion method was applied for the digestion of the 0.10 g of CRM. Digest was completed to 25.0 mL after spiking Be internal standard. Concentration of Be in the solution was 25.0 ng/mL. Direct calibration technique was used. CRM was digested in duplicate and the mean value was obtained using duplicate results. Result was found in good agreement with informative value as shown in Table 3.14.

Table 3. 14 Result of the Accuracy Check for ICP-MS

CRM	Informative, mg/kg	Found, mg/kg
BCR Human Hair	2.8 ± 0.3	2.9 ± 0.3

3.2.2.6. Calculations for Boron Concentration in Blood

For each blood sample, 150 µL from the 1000 ng/mL Be solution was spiked as an internal standard. Concentration of Be in the samples must be 25.0 ng/mL to match the standards and samples. Spiked volume of Be was calculated by assuming the densities of the digested blood samples were 1.0 g/mL and final mass was exactly 6.0 g. However, when densities of the digested blood samples were calculated using 5 different samples, it was found as 1.17 g/mL. In Table 3.15, weights of 1.0 mL blood and final solution, ICPS of ^{11}B and ^{9}Be are given.

Table 3. 15 Comparison of the corrected and uncorrected ICPS

Sample code	Weight of blood, g	Weight of final solution, g	ICPS of ^{11}B	ICPS of ^{9}Be	B concentration in blood, ng/g
S47	0.9637	6.01835	4927507	1454215	140.9±4.6
C53	0.94731	6.32556	1476181	1415785	30.2±1.0
C53, corrected	0.94731	6.32556	1476181	**1492814**	**27.4±0.9**

At the beginning, calculations were made ignoring the real density of blood and assuming that it is 1.0 g/mL.

Concentration of Be in final solution of sample S47;

From $M_1 \times V_1 = M_2 \times V_2$

1000 ng/mL Be × 0.15 mL= M_2 × 6.02 mL

M_2= 24.92 ng/mL Be

Concentration of Be was 24.92 ng/mL instead of 25.0 ng/mL .When percent error was calculated, 0.33% error was found. Since this was relatively small, it could be ignored and concentration of Be in the sample was considered as 25.0 ng/mL. So, after calculating the B concentration in approximately 6-fold diluted sample from calibration graph, value was multiplied by 6.02 and then divided to initial mass, 0.964. Lastly, result was divided to 1.17 g/mL (density of the digested blood) to convert the unit to ng/g.

On the other hand, when Be concentration of sample C53 was calculated, significant difference was obtained.

Concentration of Be in final solution of sample C53,

From $M_1 \times V_1 = M_2 \times V_2$

1000 ng/mL Be$\times$ 0.15 mL= $M_2 \times$ 6.33 mL

M_2= 23.70 ng/mL Be

5.2% error was calculated for this case. When this error was compared to 0.33%, there was a big difference and this difference was significant. Therefore, for sample C53, ICPS of Be was corrected for 25.0 ng/mL Be by proportioning the Be concentrations.

ICPS of ^{9}Be	1415785	for	23.70 ng/mL Be
ICPS of ^{9}Be	*1492814*	for	25.0 ng/mL Be

Then, ^{11}B to ^{9}Be ratio was calculated by using new ICPS of Be. Rest of the calculations was similar to the calculations of sample S47.

In conclusion, when calculating the B concentrations of blood samples, if the error exceeded the 5.0% for Be concentration, correction was done as it was the case for C53.

3.2.2.7. Boron Concentrations of the Urine and Blood Samples

For this study, in total 258 urine and 204 blood samples were analyzed. Among 258 urine samples, 54 of them were from Bigadiç region whereas rests were from Bandırma region. The boron concentrations of urine samples from Bigadiç and Bandırma regions are listed in Table 3.16 and 3.17, respectively. Each group included both control and study groups. Two parallel samples were analyzed for each urine sample. Average of the two results was given as the final results.

Table 3. 16 Boron concentrations of the urine samples from Bigadiç region

Control Group	B, mg/L
C-1	0.48±0.02
C-2	*1.86±0.08*
C-3	0.37±0.01
C-4	0.47±0.02
C-5	0.73±0.03
C-6	1.81±0.08
C-7	1.19±0.05
C-8	0.67±0.03
C-9	1.13±0.05
C-10	0.50±0.02
C-11	1.00±0.05
C-12	1.45±0.07
C-13	0.94±0.04
C-14	1.03 ±0.05
C-15	1.14±0.05

Study Group	B, mg/L
S-1	4.94±0.23
S-2	2.46±0.11
S-3	2.31±0.11
S-4	3.71±0.17
S-5	2.41±0.11
S-6	5.11±0.23
S-7	2.00±0.09
S-8	3.33±0.15
S-9	4.41±0.20
S-10	3.51±0.16
S-11	3.70±0.17
S-12	4.10±0.19
S-13	2.97±0.14
S-14	5.17±0.24
S-15	3.08±0.14

Table 3.16 Continued

C-16	0.55±0.02
C-17	0.71±0.03
C-18	0.93±0.04
C-19	1.34±0.06
C-20	0.78±0.04
C-21	0.48±0.02
C-22	0.68±0.03
C-23	0.96±0.04
C-24	0.85±0.04
C-25	*0.34±0.02*
C-26	1.02±0.05

S-16	*5.88±0.27*
S-17	4.82±0.22
S-18	2.88±0.13
S-19	2.34±0.11
S-20	2.24±0.10
S-21	2.87±0.13
S-22	*1.66±0.08*
S-23	4.99±0.23
S-24	3.08±0.14
S-25	2.54±0.12
S-26	4.29±0.20
S-27	2.56±0.12
S-28	4.18±0.19

Table 3. 17 Boron concentrations of the urine samples from Bandırma region

Control Group	**B, mg/L**
C-1	4.35±0.34
C-2	9.03±0.04
C-3	3.65±0.36
C-4	1.37±0.13
C-5	4.32±0.05
C-6	1.37±0.12
C-7	0.66±0.02

Study Group	**B, mg/L**
S-1	3.42±0.22
S-2	3.53±0.26
S-3	5.46±0.20
S-4	1.22±0.09
S-5	9.76±1.20
S-6	6.37±0.15
S-7	4.47±0.04

Table 3.17 Continued

C-8	5.95±0.42	S-8	3.86±0.44
C-9	0.70±0.02	S-9	3.00±0.14
C-10	*0.36±0.01*	S-10	2.88±0.14
C-11	3.19±0.17	S-11	1.46±0.02
C-12	1.81±0.16	S-12	5.53±0.76
C-13	N.D	S-13	1.01±0.02
C-14	1.53±0.02	S-14	11.9±0.2
C-15	0.70±0.07	S-15	9.81±0.27
C-16	6.70±0.29	S-16	9.28±0.21
C-17	3.74±0.10	S-17	8.42±0.53
C-18	4.78±0.10	S-18	13.4±1.4
C-19	5.27±0.33	S-19	14.3±0.5
C-20	2.17±0.04	S-20	1.82±0.04
C-21	5.91±0.31	S-21	6.58±0.01
C-22	2.95±0.11	S-22	12.3±0.1
C-23	0.98±0.04	S-23	16.2±0.7
C-24	1.09±0.12	S-24	11.3±1.0
C-25	4.37±0.09	S-25	4.42±0.16
C-26	5.64±0.39	S-26	5.07±0.03
C-27	5.25±0.49	S-27	11.0±0.2
C-28	10.5±0.10	S-28	10.5±1.0
C-29	7.05±0.09	S-29	11.6±1.3
C-30	1.89±0.15	S-30	6.84±0.02
C-31	11.5±0.6	S-31	3.85±0.23
C-32	3.12±0.06	S-32	3.00±0.03

Table 3.17 Continued

C-33	3.24±0.15		S-33	9.89±0.22
C-34	9.54±0.41		S-34	13.4±0.7
C-35	1.64±0.11		S-35	2.23±0.10
C-36	2.21±0.11		S-36	2.70±0.08
C-37	3.67±0.01		S-37	12.0±0.5
C-38	2.11±0.13		S-38	1.55±0.11
C-39	1.24±0.02		S-39	2.96±0.17
C-40	0.55±0.01		S-40	2.76±0.15
C-41	3.62±0.15		S-41	3.21±0.02
C-42	6.12±0.29		S-42	6.73±0.05
C-43	1.34±0.10		S-43	6.35±0.23
C-44	1.75±0.07		S-44	9.78±0.17
C-45	2.75±0.14		S-45	3.57±0.11
C-46	3.46±0.19		S-46	8.38±0.50
C-47	1.60±0.19		S-47	13.6±0.6
C-48	1.70±0.09		S-48	11.6±0.3
C-49	4.90±0.44		S-49	1.71±0.07
C-50	2.82±0.04		S-50	6.33±0.15
C-51	9.99±0.10		S-51	8.04±0.19
C-52	6.50±0.23		S-52	12.0±0.4
C-53	1.36±0.04		S-53	11.6±0.8
C-54	3.28±0.04		S-54	3.41±0.03
C-55	1.62±0.10		S-55	1.12±0.07
C-56	2.53±0.20		S-56	2.72±0.10
C-57	3.49±0.13		S-57	6.47±0.48

Table 3.17 Continued

C-58	5.44±0.65	S-58	14.5±0.5
C-59	3.28±0.18	S-59	12.4±0.2
C-60	9.21±0.37	S-60	8.33±0.05
C-61	*12.3±0.3*	S-61	5.25±0.31
C-62	0.71±0.02	S-62	2.75±0.02
C-63	1.65±0.15	S-63	6.40±0.14
C-64	9.36±0.25	S-64	2.51±0.09
C-65	7.73±0.29	S-65	*0.57±0.03*
C-66	3.83±0.22	S-66	2.91±0.18
C-67	6.87±0.13	S-67	2.85±0.20
C-68	0.65±0.07	S-68	7.72±0.55
C-69	2.17±0.19	S-69	6.16±0.45
C-70	1.26±0.06	S-70	5.58±0.25
C-71	0.75±0.06	S-71	7.33±0.13
C-72	3.96±0.33	S-72	6.14±0.45
C-73	5.05±0.17	S-73	6.23±0.80
C-74	0.43±0.08	S-74	2.40±0.03
C-75	1.97±0.02	S-75	1.54±0.03
C-76	4.21±0.12	S-76	8.54±1.02
C-77	6.41±0.15	S-77	3.44±0.03
C-78	2.31±0.11	S-78	3.64±0.06
C-79	1.36±0.05	S-79	1.92±0.09
C-80	1.07±0.16	S-80	13.0±0.1
C-81	2.41±0.31	S-81	5.83±0.16
C-82	3.83±0.22	S-82	5.34±0.07

Table 3.17 Continued

C-83	4.97±0.41	S-83	14.0±0.7
C-84	5.40±0.43	S-84	7.77±0.27
C-85	1.52±0.01	S-85	2.71±0.04
C-86	4.64±0.19	S-86	3.16±0.07
C-87	11.3±0.9	S-87	16.6±1.1
C-88	3.47±0.07	S-88	9.04±0.46
C-89	10.1±0.6	S-89	5.02±0.62
C-90	7.19±0.13	S-90	16.5±0.6
C-91	3.61±0.34	S-91	6.48±0.03
C-92	1.94±0.11	S-92	9.22±0.65
C-93	2.68±0.06	S-93	4.01±0.13
C-94	N.D	S-94	1.40±0.01
C-95	3.85±0.03	S-95	1.59±0.01
C-96	4.97±0.10	S-96	3.34±0.08
C-97	7.64±0.29	S-97	2.89±0.03
C-98	5.51±0.45	S-98	7.22±0.14
C-99	1.45±0.05	S-99	11.1±1.2
C-100	0.65±0.01	S-100	1.41±0.16
C-101	4.76±0.09	S-101	*16.7±1.0*
C-102	1.93±0.21	S-102	1.97±0.13

Results of the 204 blood samples were listed in Table 3.18. In contrast to urine samples, all blood samples were not analyzed in two replicates. For each 25 samples, one sample with three replicates was analyzed and relative standard deviation (RSD) of the results was applied to other samples.

Table 3. 18 Boron concentrations of the blood samples from Bandırma region

Control Group	B, ng/g
C-1	58.7±2.0
C-2	85.6±3.0
C-3	N.D
C-4	35.4±1.2
C-5	40.5±1.4
C-6	N.D
C-7	N.D
C-8	66.6±2.3
C-9	92.5±3.2
C-10	27.7±1.0
C-11	96.7±1.5
C-12	42.6±1.5
C-13	N.D
C-14	117.6±4.1
C-15	111.5±3.9
C-16	69.0±2.4
C-17	72.1±2.5
C-18	76.6±2.7
C-19	58.9±2.1
C-20	105.4±3.7
C-21	67.7±2.4
C-22	116.9±4.1
C-23	94.0±3.3
C-24	30.7±1.1

Study Group	B, ng/g
S-1	164.2±5.7
S-2	48.6±1.7
S-3	104.9±3.6
S-4	71.8±2.5
S-5	194±6.7
S-6	62.6±2.2
S-7	94.1±3.3
S-8	95.5±3.1
S-9	121.0±4.2
S-10	381.9±13.2
S-11	80.1±2.8
S-12	404.4±14.0
S-13	255.7±8.9
S-14	288.2±10.0
S-15	197.2±6.8
S-16	98.1±3.4
S-17	151.7±5.3
S-18	205.5±3.7
S-19	160.8±5.6
S-20	234.4±8.1
S-21	170.9±5.9
S-22	206.2±7.2
S-23	251.1±8.7
S-24	244.3±8.5

Table 3.18 Continued

C-25	25.7±0.9	S-25	111.6±3.9
C-26	84.7±2.9	S-26	126.9±4.4
C-27	71.9±2.5	S-27	161.8±5.6
C-28	202.7±7.0	S-28	197.9±6.9
C-29	178.8±6.2	S-29	335.2±11.6
C-30	42.5±1.5	S-30	170.0±5.9
C-31	102.6±3.6	S-31	*531.2±18.4*
C-32	57.2±2.0	S-32	45.6±1.6
C-33	118.3±4.1	S-33	316.7±11.0
C-34	119.9±4.2	S-34	140.4±4.9
C-35	112.0±3.9	S-35	185.4±6.4
C-36	145.0±5.0	S-36	96.8±3.4
C-37	86.3±3.0	S-37	109.7±3.8
C-38	27.2±0.9	S-38	45.1±1.6
C-39	26.8±0.9	S-39	133.0±4.6
C-40	22.0±0.8	S-40	99.7±3.5
C-41	150.0±5.0	S-41	88.6±3.1
C-42	57.6±2.0	S-42	205.8±7.1
C-43	63.5±2.2	S-43	229.8±8.0
C-44	21.8±0.8	S-44	164.5±5.7
C-45	103.0±3.6	S-45	126.9±4.4
C-46	74.4±2.6	S-46	94.5±3.3
C-47	109.0±3.8	S-47	236.8±8.2
C-48	62.7±2.2	S-48	164.9±5.7
C-49	110.6±3.8	S-49	213.2±7.4

Table 3.18 Continued

C-50	93.2±3.2	S-50	148.1±5.1
C-51	127.7±4.4	S-51	127.6±4.4
C-52	76.6±2.7	S-52	126.1±4.4
C-53	32.1±1.1	S-53	255.5±8.9
C-54	33.4±1.2	S-54	155.9±5.4
C-55	28.6±1.0	S-55	298.9±10.4
C-56	*20.2±0.7*	S-56	208.3±7.2
C-57	81.6±2.8	S-57	185.9±6.4
C-58	21.2±0.7	S-58	223.8±7.8
C-59	36.9±1.3	S-59	319.2±11.1
C-60	128.8±4.5	S-60	118.5±4.1
C-61	142.4±4.9	S-61	249.2±8.6
C-62	100.2±3.5	S-62	96.1±3.3
C-63	N.D	S-63	41.4±1.4
C-64	93.2±3.2	S-64	80.0±3.2
C-65	147.1±5.1	S-65	43.7±1.5
C-66	45.8±1.6	S-66	103.0±3.6
C-67	52.1±1.8	S-67	29.9±1.0
C-68	N.D	S-68	70.8±2.5
C-69	56.7±2.0	S-69	70.3±2.4
C-70	68.3±2.4	S-70	120.6±4.2
C-71	24.5±0.9	S-71	88.2±3.1
C-72	37.5±1.3	S-72	119.0±4.1
C-73	N.D	S-73	110.8±3.8
C-74	N.D	S-74	102.7±3.6

Table 3.18 Continued

C-75	*294.8±10.2*	S-75	128.6±4.5
C-76	33.8±1.2	S-76	*29.5±1.0*
C-77	92.0±3.2	S-77	97.2±3.4
C-78	116.9±4.1	S-78	123.6±4.3
C-79	84.1±2.9	S-79	129.6±4.5
C-80	63.4±2.2	S-80	119.4±4.1
C-81	164.9±5.7	S-81	161.5±5.6
C-82	42.6±1.5	S-82	469.9±16.3
C-83	38.3±1.3	S-83	211.9±7.3
C-84	65.0±2.3	S-84	341.4±11.8
C-85	23.0±0.8	S-85	249.2±8.6
C-86	46.3±1.6	S-86	158.4±5.5
C-87	184.1±6.4	S-87	136.4±4.7
C-88	29.5±1.0	S-88	185.7±6.8
C-89	201.2±7.0	S-89	166.8±5.8
C-90	59.2±2.1	S-90	93.1±3.2
C-91	54.8±1.9	S-91	334.3±11.6
C-92	32.8±1.1	S-92	118.5±4.1
C-93	42.4±1.5	S-93	147.1±5.1
C-94	37.5±1.3	S-94	155.8±5.4
C-95	38.6±1.3	S-95	48.2±1.7
C-96	100.4±3.5	S-96	71.6±2.5
C-97	153.1±3.3	S-97	160.4±5.6
C-98	60.3±2.1	S-98	170.6±5.9
C-99	89.6±3.1	S-99	75.0±2.6

Table 3.18 Continued

C-100	61.4±2.1
C-101	63.1±2.2
C-102	48.9±0.3

S-100	116.0±4.0
S-101	68.5±2.4
S-102	306.6±10.6

For urine and blood samples, concentrations of boron for study group were higher than the control group as it is expected.

For urine analysis, B concentration range of the Study Group was between 1.66 mg/L and 5.88 mg/L while that of Control Group was between 0.34 mg/L and 1.86 mg/L for Bigadiç region. On the other hand, range was wider for the results of the Bandırma region. For Control Group 0.36 mg/L was the lowest boron concentration and 12.3 mg/L was the highest one. The more meaningful results were the mean and median values which were 3.91 and 3.37 mg/L, respectively. However, boron concentrations of the Study Group were between 0.57 and 16.7 mg/L. Mean value for this group was 6.60 mg/L whereas median was 5.98 mg/L.

For blood samples, minimum concentrations that could be quantified were 20.2 ng/g and 29.5 ng/g for Control and Study Groups, respectively. 294.8 ng/g was obtained as maximum for Control Group while 531.2 ng/g was the maximum of the Study Group. When mean values were calculated, 78.9 ng/g and 163.6 ng/g were obtained for Control and Study Group, respectively.

According to the results of a study by *Sun et al.*, B concentrations of two human urine samples were found to be approximately 1.0 mg/L. On the other hand, concentrations of B in two human serum and plasma samples were in the range of 32.8-38.8 ng/mL [61]. These subjects had not been exposed to high levels of boron and thus the results could be accepted as control values.

In order to check statistically whether the mean values of the Control Group and Study Group were significantly different than each other, Independent-Samples t-test was applied. This test is used when mean scores of two different groups of people are compared [79]. Control Group and Study Group of each region were compared. SPSS 15.0 for Windows software was used in computations.

For Bigadiç region, mean and standard deviation values of the Study and Control Groups are shown in Table 3.19.

Table 3. 19 Group Statistics for urine samples from Bigadiç region

	groups	**N**	**Mean, mg/L**	**Std. Deviation**	**Std. Error of Mean**
Urine	**Control**	26	0.9004	0.40426	0.07928
	Study	28	3.4836	1.13752	0.21497

The results of the independent-sample t-test for Bigadiç region are given in Table 3.20. Results are evaluated by considering the 95% confidence interval of the difference. The first section of the output table gives the results of Levene's test for equality of variances. This test checks whether the variance of scores for the Study and Control Groups is the same. If significance level (Sig.) is smaller than 0.05, it means equal variances are not assumed and information in the second row of the table will be used. Then, to find out if there is a significant difference between groups, Sig (2-tailed) value is evaluated. In case of equal or smaller value than 0.05, there is a significant difference in the mean scores of two groups [79]. For urine samples of the Bigadiç region, this value was 0.000 so there is a significant difference in the mean values of Control and Study Groups.

Table 3. 20 Independent-sample t-test results for two groups of urine samples from Bigadiç region

		Levene's test Equality of Variances		t-test for Equality of Means						
									95% Confidence interval of the difference	
		F	Sig.	t	df	Sig. (2-tailed)	Mean Difference	Std. Error difference	Lower	Upper
Urine	Equal variances assumed	28.7	.000	-10.949	52	.000	-2.5831	.23593	-3.057	-2.109
	Equal variances not assumed			-11.274	34.162	.000	-2.5831	.22912	-3.049	-2.117

Next, independent-sample t-test was applied for the urine samples from Bandırma region. Before forming the output table, five results from the Control Group were removed since they were outliers. Removed values belonged to samples coded as C-28, C-31, C-61, C-87 and C-89, respectively. For the rest, mean and standard deviation values of the Study and Control Groups are shown in Table 3.21.

Table 3. 21 Group Statistics for urine samples from Bandırma region

	groups	**N**	**Mean, mg/L**	**Std. Deviation**	**Std. Error of Mean**
Urine	**control**	95	3.5266	2.36623	0.24277
	study	102	6.5988	4.30017	0.42578

The results of the independent-sample t-test for this region are given in Table 3.22.

Table 3. 22 Independent-sample t-test results for two groups of urine samples from Bandırma region

		Levene's test Equality of Variances		t-test for Equality of Means						
									95% Confidence interval of the difference	
		F	Sig.	t	df	Sig. (2-tailed)	Mean Difference	Std. Error difference	Lower	Upper
Urine	Equal variances assumed	36.9	.000	-6.149	195	.000	-3.07219	.49959	-4.058	-2.087
	Equal variances not assumed			-6.268	159.26	.000	-3.07219	.49013	-4.040	-2.104

Similar to Bigadiç region, Sig. (2-tailed) value of the second row was evaluated. Since 0.000 value is smaller than 0.05, it was concluded that there is a significant difference between the mean values of Control and Study Groups.

Lastly, mean values of the two groups were compared for blood samples. Before obtaining the output table, four values from Study Group and also three values of Control Group were removed because they were defined as outliers. C-28, C-75 and C-89 were the outliers for Control Group while S-10, S-12, S-31 and S-82 were the outliers for Study Group. Mean and standard deviation values of both groups are shown in Table 3.23.

Table 3. 23 Group Statistics for blood samples from Bandırma region

	groups	**N**	**Mean, ng/g**	**Std. Deviation**	**Std. Error of Mean**
Blood	**control**	91	73.7831	39.8668	4.17918
	study	98	152.042	75.5053	7.62719

Outputs of the independent-sample t-test for blood samples are given in Table 3.24.

Table 3. 24 Independent-sample t-test results for two groups of blood samples from Bandırma region

		Levene's test Equality of Variances		t-test for Equality of Means						
									95% Confidence interval of the difference	
		F	Sig.	t	df	Sig. (2-tailed)	Mean Difference	Std. Error difference	Lower	Upper
Blood	Equal variances assumed	28.3	.000	-8.811	187	.000	-78.25876	8.88167	-95.78	-60.74
	Equal variances not assumed			-8.998	149.47	.000	-78.25876	8.69710	-95.44	-2.104

As it can be seen, Sig. (2-tailed) value of the second row is 0.000. This indicates that there is a significant difference in mean values of Control and Study Groups.

To sum up, for urine samples from both regions and also for blood samples, mean values of the Control Group and Study Group are significantly different from each other at 95% confidence level.

CHAPTER 4

CONCLUSIONS

In this study, the main purpose was the development of a sensitive analytical method for boron determination in blood samples by ICP-MS. Then, the previously developed method by our research group and this new one were used to analyze the urine and blood samples, respectively.

Before the analysis of urine samples, robustness test was applied for ICP-OES and optimum values of the operating parameters were selected. Urine samples were digested in microwave oven with the addition of 5.0 mL distilled concentrated HNO_3. Indium was used as internal standard. The wavelength was 249.773 nm for B. 230.606 nm emission line gave the best signal for In determination. LOD (3s/m) and LOQ (10s/m) values of B for this method were calculated as 0.021 mg/L and 0.070 mg/L, respectively. Accuracy check of the method was performed by using the NIST 1573a Tomato Leaves as standard reference material and result for B was in good agreement with the certified value.

For boron determination by ICP-MS, first problem was the memory effect. In order to eliminate this problem, 0.25% (w/v) mannitol and 0.10 M ammonia mixture was used as a wash solution after each solution once. This mixture helped to eliminate memory effect. However, since there were 204 blood samples to be analyzed, this was a very time-consuming method. So, a new sample introduction system which consists of perfluoroalkoxy (PFA) spray chamber and nebulizer and also alumina (Al_2O_3) injector tube of the torch was used for this study.

Digestion of the blood samples was necessary in order to prevent the blockage of orifices of sampler and skimmer cones due to high organic content. Therefore, microwave digestion was applied to blood samples. According to optimized digestion procedure, approximately 1.0 g blood samples were digested by the addition of 2.0 mL concentrated distilled HNO_3 and 2.0 mL concentrated H_2O_2. The test solution was approximately 6.0 g after spiking Be to provide minimum dilution of the sample.

Be was used as an internal standard for boron determination by ICP-MS due to its similar mass number and ionization potential to boron. During the method development, both ^{10}B and ^{11}B were evaluated. The interference effect of beryllium on ^{10}B signal by forming BeH^+ was shown to be not possible.

Signals of ^{11}B were used during the method development and analysis of blood samples since sensitivity of ^{11}B is 4 times better than that of ^{10}B.

Due to their small masses, in the plasma boron and beryllium are affected from heavier elements such as Na, of which concentration in blood is 0.3105-0.3404% (w/v). Space charge effect of Na^+ ion was investigated for this study and it was concluded that the $^{11}B/^{9}Be$ ratio was suppressed less than $^{10}B/^{9}Be$ ratio for the same concentration of Na in the test solution. Moreover, % decrease was below 5.0 for $^{11}B/^{9}Be$. So, no further study was done with Na since 3.0% decrease was accepted as tolerable. In addition, effectiveness of using Be internal standard was proven since % change decreased to 3.0% for $^{11}B/^{9}Be$ ratio while it was 39.0% for ^{11}B.

Apart from Na space charge effect, carbon interference on B and Be signals in both spectral and non-spectral respects were studied. Ionization potentials are related to non-spectral interference effect of carbon. According to TOC results of six different blood samples, carbon concentrations of undigested blood were found to be 9-11% (w/v) while that of microwave digested blood was reduced to 1.4-4.3% (w/v). To check the effect of C, sugar was added to the standard solutions with increasing

concentrations. As C concentration increased, B and Be signals increased, but not similarly. Approximately 0.4% (w/v) C which was present in the final solution of the blood samples corresponds to 1.0% (w/v) sugar. Therefore, 1.0% (w/v) sugar was added into calibration standards to compensate for this difference for blood analysis.

Elimination of carbon from the sample is a better solution than matching the matrix, so carbon elimination studies were performed. With open-digestion, carbon was removed from the samples approximately 3 times more efficiently than with the microwave digestion. However, open-digestion is not a preferred digestion procedure due to the risk of boron vaporization. In addition, UV radiation was used to eliminate C and 38% decrease was obtained by this process when exposure time was 3 hours. However, more effective methods must be developed for the maximum reduction or complete elimination of carbon with easy application to large number of samples. Both open digestion and UV irradiation help to reduce carbon content but for a large number of analyses these procedures are not practicable. Therefore, these approaches of C elimination were not applied for this study.

When results of the samples were considered, as it is expected and proven by SPSS program B concentrations of the study group was higher than the control group for both urine and blood samples. For urine samples, higher boron concentrations were obtained from the samples of the Bandırma region since study group of this region consists of the people who work at the boric acid factory. Apart from getting boron via foods and drinking water, they were also exposed to boron via inhalation. Situation was the same for the blood samples and concentrations of the boron in the blood of the study group were much higher than the control group that live near to the boric acid factory but not work at the factory.

After all, developed method can be used for boron determination in blood samples by ICP-MS trustfully. Moreover, obtained results will be used to relate the exposed concentrations and the possible risk of the diseases. Results of this study can also be helpful to determine reference value for the safe upper limit of boron intake.

REFERENCES

1. P. Argust, Distribution of boron in the environment, *Biol. Trace Elem. Res.* 66, 1998, 131-143.
2. A. A. Nemodruk, Z. K. Karalova, *Analytical chemistry of boron*, 1964.
3. R. G.Downing, P. L. Strong, Analytical Challenges of Low Level Boron Analysis in Biological Matrices, *J. Trace Elem. Exp. Med.* 12, 1999, 205-212.
4. P. P. Power, W. G. Woods, The chemistry of boron and its speciation in plants, *Plant and Soil* 193, 1997, 1-13.
5. N. Acarkan, Boron products and their uses, *Proceedings of the 1st international boron symposium*, October 3-4, 2002.
6. I. Özpeker, Valuation of boron reserves, *Proceedings of the 1st international boron symposium,* October 3-4, 2002.
7. H. Hu, P. H. Brown, Absorption of boron by plant roots, *Plant and Soil* 193, 1997, 49-58.
8. T. Matoh, Boron in plant cell walls, *Plant and Soil* 193, 1997, 59-70.
9. I. Çakmak, V. Romheld, Boron Deficiency-induced impairments of cellular functions in plants, *Plant and Soil* 193, 1997, 71-83.
10. B. Dell, L. Huang, Physiological response of plants to low boron, *Plant and Soil* 193, 1997, 103-120.
11. W. G. Woods, A review of possible boron speciation relating to its essentiality, *J. Trace Elem. Exp. Med* 9, 1996, 153-163.
12. R. N. Sah, P. H. Brown, boron determination- A review of analytical methods, Microchem. J. 56, 1997, 285-304.
13. R. O. Nable, G. S. Banuelos, J.G. Paull, Boron Toxicity, *Plant and Soil* 193, 1997, 181-198.
14. F. H. Nielsen, Boron in human and animal nutrition, *Plant and Soil* 193, 1997, 199-208.

15. C. D. Hunt, The biochemical effects of physiological amounts of dietary boron in animal nutrition models, *Environ. Health Perspect.* 102 suppl 7, 1994, 35-43.
16. F. H. Nielsen, L. M. Mullen, S. K. Gallagher, Effect of boron depletion and repletion on blood indicators of calcium status in humans fed a magnesium-low diet, *J. Trace Elem. Exp. Med* 3, 1990, 45-54.
17. J. G. Penland, Dietary boron, brain function and cognitive performance, *Environ. Health Perspect.*102 suppl 7, 1994, 65-72.
18. Y. Bai, C. D. Hunt, Dietary boron increases serum antibody concentrations in rats immunized with heat-killed mycobacterium tuberculosis (MT), *FASEB* 10, 1996b, A 819.
19. B. Sutherland, R. Leslie, P.S. Woodhouse, C.K. Janet, Boron balance in humans, *J. Trace Elem. Exp. Med* 12, 1999, 271-284.
20. B.D. Culver, P.T. Shen, T.H. Taylor, A. Lee-Feldstein, H. Anton-Culver, P.L. Strong, The relationship of blood- and urine-boron to boron exposure in the borax-workers and usefulness of urine-boron as an exposure marker, *Environ. Health Perspect.* 102(Suppl. 7), 1994,133–137.
21. C. D. Hunt, Boron, In Encyclopedia of Food Science, *Food Technology and Nutrition 1*, Academic Press, London, 1993, 440-447.
22. W. W. Ku, R. E. Chapin, R. N. Wine, B.C. Gladen, Testicular toxicity of boric acid (BA): relationship of dose to lesion development and recovery in the F344 rat, *Reproduct. Toxicol.* 7, 1993, 305-319.
23. R. J. Weir, R. S. Fisher, Toxicologic studies on borax and boric acid, *Toxicol. Appl. Pharmacol.* 23, 1972, 351-364.
24. B. S. Şaylı, E. Tüccar, A.H. Elhan, An Assessment of Fertility in Boron-Exposed Turkish Subpopulations, *Reproduct. Toxicol* 12,1998, 297-304.
25. B. S. Şaylı, An Assessment of Fertility in Boron-Exposed Turkish Subpopulations 2: evidence that boron has no effect on human reproduction, *Biol. Trace Elem. Res.* 66, 1998, 409-422.

26. B. S. Şaylı, An Assessment of Fertility in Boron-Exposed Turkish Subpopulations 3: evaluation of fertility among sibs and in "borate families", *Biol. Trace Elem. Res.* 81, 2001, 255-267.
27. B. S. Şaylı, Low frequency of infertility among workers in a borate processing facility, *Biol. Trace Elem. Res.* 93, 2003, 19-29.
28. J.J. Heindel, C.J. Price, E.A.Field, M.C. Marr, C.B. Myers, R.E. Morrissey, B.A. Schwetz, Developmental toxicity of boric acid in mice and rats, *Fund. Appl. Toxicol.* 18, 1992, 266-277.
29. C.J. Price, M.C. Marr, C.B. Myers, J.C. Seely, J.J. Heindel, B.A. Schwetz, The developmental toxicity of boric acid in rabbits, *Fund. Appl. Toxicol.* 34, 1996, 176-187.
30. Y. Cui, M. I. Winton, Z. F. Zhang, C. Rainey, J. Marshall, J. B. De Kernion, C. D. Eckhert, Dietary boron intake and prostate cancer risk, *Oncol. Rep.* 11, 2004, 887-892.
31. Z. F. Zhang, M. I. Winton, C. Rainey, C. D. Eckhert, Boron is associated with decreased risk of human prostate cancer, *FASEB* 15, 2001, 834.3.
32. M. Korkmaz, E. Üzgören, S. Bakırdere, F. Aydın, O. Y. Ataman, Effects of Dietary Boron on Cervical Cytopathology and on Micronucleus Frequency in Exfoliated Buccal Cells, *Environ. Toxicol.* , 22, 2007, 17-25.
33. WHO/FAO/IAEA: 1996, Trace elements in Human Nutrition and Health, World Health Organization, Geneva, pp 175-179.
34. B. Wolf, Improvement in the azomethine-H method for the determination of boron, *Comm. Soil Sci. Plant Anal.* 5, 1974, 39-44.
35. M. C. Rand, Standard Methods for the examination of water and wastewater, *APHA,* Washington, DC, 1975, 287-291.
36. F. J. Lopez, E. Gimenez, F. Handez, Analytical study on the determination of boron in environmental water samples, *Fresen. J. Anal. Chem*. 346, 1993, 984-987.
37. A. M. G. Campana, F. A. Barrero, M. R. Ceba, Spectrofluorimetric determination of boron in soil plants and natural waters with Alizarin red-S, *Analyst* 117, 1992, 1189-1191.

38. R. M. Carlson, J. L. Paul, Potentiometric determination of boron as tetrafluoroborate, *Anal. Chem.* 40, 1968, 1292-1295.
39. D. E. Moore, A review of techniques for the analysis of boron in the development of neutron capture therapy agents, *J. Pharmaceut. Biomed. Anal.* 8, 1990, 547-553.
40. M. Papaspyrou, L. E. Feinendegen, C. Mohl, M. J. Schwuger, Determination of boron in cell suspensions using electrothermal atomic absorption spectrometry, *J. Anal. At. Spectrom.* 9, 1994, 791-795.
41. G. M. A. Botelho, A. J. Curtius, R. C. Campos, Determination of boron by electrothermal atomic absorption spectrometry, testing different modifiers atomization surfaces and potential interferents, *J. Anal. At. Spectrom.* 9, 1994, 1263-1267.
42. M. Luguera, Y. Madrid, C. Camara, Combination of chemical modifiers and graphite tube pre-treatment to determine boron by atomic absorption spectrometry, *J. Anal. At. Spectrom.* 8, 1991, 669-672.
43. M. A. B. Pougnett, M. J. Orren, The Determination of Boron by Inductively Coupled Plasma Atomic Emission Spectroscopy. Part 1: Method Development, *Int. J. Environ. Anal. Chem.* 24, 1986, 253-266.
44. S. Evans, U. Krahenbuhl, Boron analysis in biological material: microwave digestion procedure and determination by different methods, *Fresen. J. Anal. Chem.* 349, 1994, 454-459.
45. S. Evans, U. Krahenbuhl, Improved Boron Determination in Biological Material by Inductively Coupled Plasma Mass Spectrometry, *J. Anal. At. Spectrom.* 9, 1994, 1249-1253.
46. E. Nakamura, T. Ishikawa, J. L. Birck, C. J. Allegre, Precise boron isotopic analysis of natural rock samples using a boron mannitol complex, *Chem. Geol.* 94, 1992, 193-204.
47. P. K. Chu, R. J. Bleiler, J. M. Metz, Determination of sub-parts per billion boron contamination in n+ Czochralski silicon substrates by SIMS, *J. Electrochem. Soc.* 141, 1994, 3453-3456.

48. J. K. Aggrawal, M. R. Palmer, Boron isotope analysis-A review, *Analyst* 120, 1995, 1301-1307.
49. J. Nolte, *ICP Emission Spectrometry, A Practical Guide*, 2003, Wiley-VCH
50. J. R. Dean, *Practical Inductively Coupled Plasma Spectroscopy*, 2005, John Wiley & Sons.
51. R. Thomas, *Practical Guide to ICP-MS*, 2004.
52. R. E. Wolf, Ph. D., Research Chemist, USGS/CR/CICT, March 2005.
53. J. Barker, *Mass Spectrometry,* 1998, John Wiley & Sons.
54. J. Dennaud, A. Howes, E. Poussel, J. M. Mermet, Study of ionic-to-atomic line intensity ratios for two axial viewing-based inductively coupled plasma atomic emission spectrometers, *Spectrochim. Acta* Part B, 56, 2001, 101-112.
55. S. Öztürk, Use of Solid Phase Extraction for Preconcentration of Rare Earth Elements: Provenance Studies in Catalhoyuk Obsidians, *M.Sc. Thesis*, METU (2003)
56. J. M. Mermet, Use of magnesium as a test element for inductively coupled plasma atomic emission spectrometry diagnostics, *Anal. Chim. Acta* 250, 1991, 85-94.
57. D. H. Sun, J.K. Waters, T. P. Mawhinney, Microwave digestion and Ultrasonic nebulization for determination of boron in animal tissue by inductively coupled plasma atomic emission spectrometry with internal standardization and addition of mannitol, *J. Anal. At. Spectrom.*12, 1997, 675.
58. A. S. Al-Ammar, R. K. Gupta, R. M. Barnes, Elimination of boron memory effect in inductively coupled plasma –mass spectrometry by addition of ammonia, *Spectrochim. Acta* Part B 54, 1999, 1077-1084.
59. N.I. Ward, F.R. Abou-Shakra, S.F. Durrant, Trace elemental content of biological materials A comparison of NAA and ICP-MS analysis*, Biol. Trace Elem. Res.* 26, 1990,177-187.
60. A. C. S. Bellato, M. F. Gine, A. A. Menegario, Determination of B in body fluids by isotope dilution inductively coupled mass spectrometry with direct injection nebulization, *Microchem. J.* 77, 2004, 119-122.

61. D. H. Sun, R. L. Ma, C. W. McLeod, X. R. Wang, A. G. Cox, Determination of boron in serum, plasma and urine by inductively coupled plasma mass spectrometry. Use of mannitol-ammonia as diluent and for eliminating memory effect, *J. Anal. At. Spectrom.* 15, 2000, 257-261.
62. A. Montaser, D. W. Golightly, *Inductively Coupled Plasmas in Analytical Atomic Spectrometry,* 2nd edition, VCH Publishers, Inc, 1992, 581-614.
63. H. Vanhoe, R. Dams, J. Versieck, Use of Inductively Coupled Plasma Mass Spectrometry for the Determination of Ultra-trace Elements in Human Serum, *J. Anal. At. Spectrom.* 9, 1994, 23-31.
64. J.P. Goulle, L. Mahieu, J. Castermant, N. Neveu, L. Bonneau, G. Laine, D. Bouige, C. Lacroix, Metal and metalloid multi-elementary ICP-MS validation in whole blood, plasma, urine and hair Reference values, *Forensic Sci. Int.* 153, 2005, 39-44.
65. A. S. Al-Ammar, E. Reitznerova, R. M. Barnes, Feasibility of using beryllium as internal reference to reduce non-spectroscopic carbon species matrix effect in the inductively coupled plasma-mass spectrometry determination of boron in biological samples, *Spectrochim. Acta* part B 54, 1999, 1813-1820.
66. G. Damkroger, M. Grote, E. Janßen, Comparison of sample digestion procedures for the determination of arsenic in certified marine samples using the FI-HG-AAS technique, *Fresen. J. Anal. Chem.* 357, 1997, 817-821.
67. I. Rodushkin, T. Ruth, A. Huhtasaari, Comparison of two digestion methods for elemental determinations in plant material by ICP techniques, *Anal. Chim. Acta* 378, 1999, 191-200.
68. J. R. Dean, *Atomic Absorption and Plasma Spectroscopy*, 1997, John Wiley & Sons.
69. C. Vandecasteele, H. Vanhoe, R. Dams, Inductively Coupled Plasma Mass Spectrometry of Biological Samples, *J. Anal. At. Spectrom.* 8, 1993, 781-786.
70. M. Wurfels, E. Jackwerth, M. Stoeppler, Residues from biological materials after pressure decomposition with nitric acid 1: Carbon conversion during sample decomposition, *Anal. Chim. Acta* 226, 1989, 1-17.

71. H. M. Kingston, L.B. Jassie, *Introduction to Microwave Sample Preparation, Theory and Practice*, American Chemical Society, Washington, DC 1988, 7-31.s
72. M. Korkmaz, U. Şaylı, B. S. Şaylı, S. Bakırdere, S. Titretir, O. Y. Ataman, S. Keskin, Estimation of human daily boron exposure in a boron-rich area, *Br. J. Nutr.* 98, 2007, 571-575.
73. T. U. Probst, N. G. Berryman, P. Lemmen, L. Weissfloch, T. Auberger, D. Gabel, J. Carlsson, B. Larsson, Comparison of Inductively Coupled Plasma Atomic Emission Spectrometry and Inductively Coupled Plasma Mass Spectrometry with Quantitative Neutron Capture Radiography for the Determination of Boron in Biological Samples From Cancer Therapy, *J. Anal. At. Spectrom.*12, 1997, 1115-1122.
74. S. D. Tanner, Characterization of Ionization and matrix suppression in Inductively Coupled "Cold" Plasma Mass Spectrometry, *J. Anal. At. Spectrom.* 10, 1995, 905-921.
75. P. M. Yip, M. K. Chan, N. Zielinski, K. Adeli, Heparin interference in whole blood sodium measurements in a pediatric setting, *Clin. Biochem.* 39, 2006, 391-395.
76. S. D'Auria, M.Rossi, P. Herman, J.R. Lakowicz, Pyruvate kinase from the Thermophilic eubacterium Bacillus acidocaldarius as probe to monitor the sodium concentrations in the blood, *Biophys. Chem.* 84, 2000, 167-176.
77. M. Pettine, B. Casentini, D. Mastroianni, S.Capri, Dissolved inorganic carbon effect in the determination of arsenic and chromium in mineral waters by inductively coupled plasma-mass spectrometry, *Anal. Chim. Acta* 599, 2007, 191-198.
78. A. Bazzi, J. O. Nriagu, M. C. Inhorn, A. M. Linder, Determination of antimony in human blood with inductively coupled plasma-mass spectrometry, *J. Environ. Monit.* 7, 2005, 1251-1254.
79. J. Pallant, *SPSS Survival Manual*, 2001, Open University Press.